

Final technical report for the U Excel project

**Title: “Role of non-canonical function of ribosomal proteins in inflammation”
(BT/410/NE/U-Excel/2013)**

PI: Dr. Rupak Mukhopadhyay
Department of Molecular Biology and Biotechnology
Tezpur University
Assam 784 028

Progress Report for R&D Projects [Final]*

Section-A: Project Details

A1. Project Title: Role of non-canonical function of ribosomal proteins in inflammation

A2. DBT Sanction Order No. & Date: BT/410/NE/U-Excel/2013 dt 06 Feb, 2014

A3. Name of Principal Investigator: Dr. Rupak Mukhopadhyay

Name of Co-PI/Co-Investigator: N/A

A4. Institute: Tezpur University, Assam

A5. Address with Contact Nos. (Landline & Mobile) & Email: Department of Molecular Biology and Biotechnology, Tezpur University, PO-Napaam, Dist.-Sonitpur, Assam 784028. Phone: 03712-275417 (Office), 09954471591 (Mobile), Email: mrupak@tezu.ernet.in; mrupak@gmail.com

A6. Total Cost: Budget sanctioned: 152.07 Lakhs; Received: 146.5 Lakhs

A7. Duration: Three Years + extension

A8. Approved Objectives of the Project:

Objective 1: To study the transcriptomics profile of ribosomal proteins during inflammation

Objective 2: To study extra-ribosomal localization of ribosomal proteins during inflammation

Objective 3: To study the interaction of selected RPs with p53 during induction of inflammation in pathological conditions.

Section-B: Scientific and Technical Progress

B1. Progress made against the Approved Objectives, Targets & Timelines during the Reporting Period (1000-1500 words for interim reports; 2500-3500 words for final report; data must be included in the form of up to 3 figures and/or tables for interim reports; up to 7 figures and/or tables for final reports):

Establishment of the working model- THP1 monocytes were maintained in liquid RPMI 1640 supplemented with 2 mM glutamine, 10% FBS and penicillin/streptomycin (100 units/ml, 100 µg/ml), at 37°C in 5% CO₂ atmosphere. Cells were sub-cultured at 2 days interval at 2×10^5 cells/ml seeding density. Cells were differentiated using phorbol myristated 13-acetate (PMA) treatment at the concentration of 5 ng/ml for 48 hrs in complete media at cell density of 0.5×10^6 cells/well of a 6-well plate. After 48 hrs, PMA containing media was removed and cells were washed with Dulbecco's Phosphate Buffered Saline (DPBSA) for two times and replenished with complete RPMI1640 media and rest it for another 24 hrs (Figure 1a). Conversion of macrophages from monocytes was confirmed by structural changes of cells and changes in the expression of monocyte-macrophage markers such as CD 14 and CD11b. Microscopic images showed that macrophage like shape corroborated the conversion from monocyte to macrophage (Figure 1b). CD 14 and CD11b showed higher gene expression in PMA differentiated THP1 cells. It confirmed the proper conversion of monocyte to macrophage (Figure 1c).

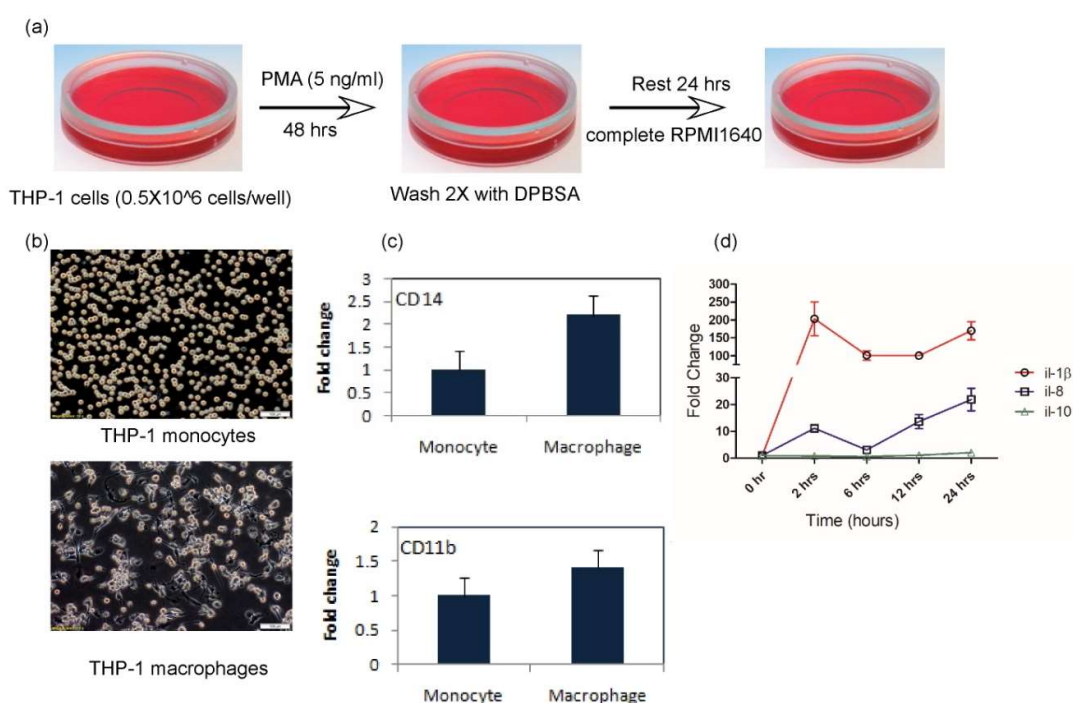


Figure 1: Establishment of *in vitro* macrophage based cell culture model. 1a. Represents treatment regime of PMA-induced conversion of THP-1 monocyte to macrophage like cells. 1b. THP-1 monocyte and macrophage like cell images were taken phase-contrast microscope (Olympus IX83, Japan) in 10X magnification. 1c. Real time PCR analysis of CD14 and CD11b genes in THP-1

monocytes and macrophages like cells. *Id. il-1 β , il-8 and il-10 genes were analyzed in LPS-treated (5 ng/ml) THP-1 macrophages up to 24 hrs by real time PCR.*

Next, we tried to understand how these PMA-differentiated THP-1 macrophages respond to bacterial lipo-polysaccharides (LPS) over different time points to inflammation. PMA differentiated THP-1 macrophages were treated with 10 ng/ml of LPS in 1% serum containing media at different time points and *il-1 β , il-8 and il-10* genes were checked using Real Time PCR (ABI7500, Applied Biosystems, USA). *il-1 β* gene showed highest expression at 2 hrs among all time points. Whereas *il-8* gene followed the same pattern as *cox2*, showed highest expression at 24 hrs of the treatment. *il-10* being an anti-inflammatory gene did not show any significant induction (Figure 1d).

Foam cell preparation- In **Objective 1**, we proposed that human monocytic cell line will be treated with LPS and oxidized LDL. The cell after accumulation of LDL becomes foam cells which are responsible for initiation of atherosclerotic plaque development leading to cardiovascular complications. To begin with, we have generated THP-1 macrophage derived foam cells. Low density lipoprotein (LDL) and CuSO₄ were purchased from Sigma Aldrich (St. Louis, USA and Merck), India respectively. LDL was oxidized using 5 μ M CuSO₄ for 24 hrs. Oxidized LDL was dialyzed using dialysis bag (molecular cut 3.5 KDa) in PBS with two time change of PBS (Figure 2a). Dialyzed ox-LDL and un-oxidized LDL were run on agarose gel electrophoresis using sodium barbital buffer to check the degree of oxidation (Figure 2b). THP-1 monocytic cells were differentiated using PMA treatment at a concentration of 5 ng/ml for 48 hrs in complete media at cell density of 0.03*10⁶ cells/well a 96 well plate. After 48 hrs, PMA-containing media was removed and cells were washed twice with DPBS, replenished with serum free RPMI-1640 media and allowed to rest for another 6 hrs. Cells were then treated with various concentration of oxidized LDL (oxLDL) (50, 100, 150, 200 and 250 μ g of ApoB100 per ml of media) for 24 hrs in serum free media. All the concentrations of oxLDL were treated in triplicate. Wells without oxLDL treatment served as control for this experiment.

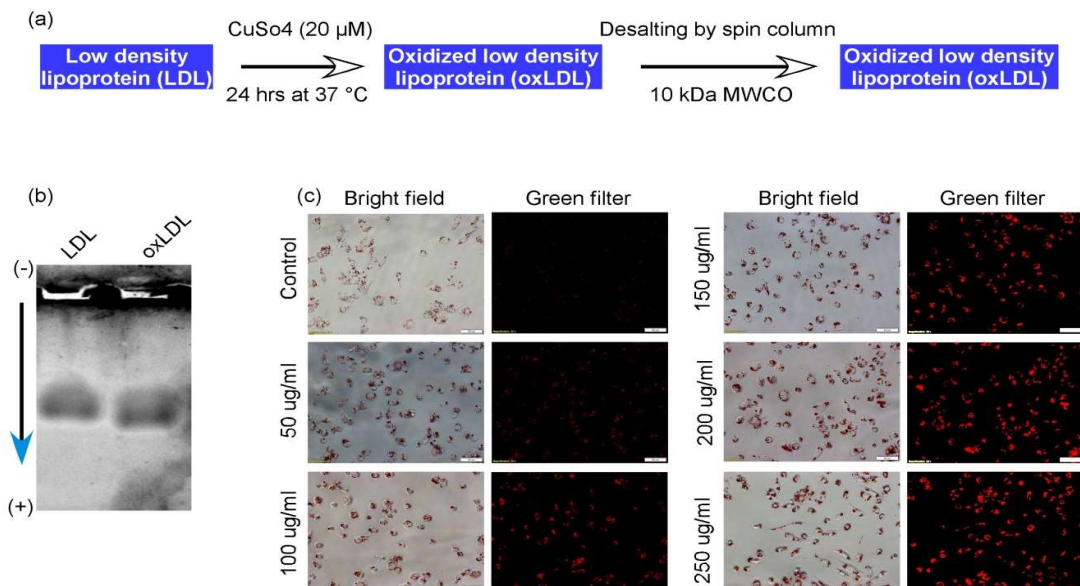


Figure 2: Preparation of THP-1 macrophage derived foam cells. 2a. Oxidation of LDL using $CuSO_4$ 2b. LDL and oxLDL were run on agarose gel in barbital buffer 2c. THP-1 macrophages were treated with increasing concentration of oxLDL (50, 100, 150, 200 and 250 $\mu\text{g/ml}$ of media). oxLDL uptake was visualized by ORO staining under bright field and green fluorescence at 20X magnification of phase contrast inverted fluorescent microscope (Olympus IX83, Japan).

Oil Red O (ORO) staining and Microscopy-After 24 hrs, media containing oxLDL was discarded and washed with ice cold PBS twice. Cells were fixed in 4% paraformaldehyde for 30 mins. Cells were washed with PBS and incubated with 60% isopropanol for 5 seconds. After washing with PBS, cells were incubated with working solution of ORO for 10 mins. ORO containing solution was discarded washed with PBS thrice. ORO staining was visualized in bright field and green filter of a phase contrast inverted fluorescence microscope. Control cells without oxLDL treatment showed basal level of fluorescence, whereas cells treated with oxLDL showed enhanced level of fluorescence. The degree of ORO uptake was seen to be in a dose-dependent manner, where lower level of fluorescence occurred in cells treated with lower doses of ox LDL (50 and 100 $\mu\text{g/ml}$) and higher level of fluorescence in cells treated with higher doses of oxLDL (200 and 250 $\mu\text{g/ml}$) (Figure 2c). Based on this result, we have selected 200 $\mu\text{g/ml}$ of oxLDL for gene expression study.

Gene expression profile of foam cells under inflammatory challenge- THP1 macrophages treated with 200 $\mu\text{g/ml}$ of oxLDL were subjected to further treatment with either IL6 (50 and 100 ng/ml) or LPS (250 and 500 ng/ml) for 2 hrs and 12 hrs. PMA-treated THP1 macrophage cells served as control for this experiment and cells treated with either IL6 or LPS served as positive control for inflammation induction. Neither concentration of IL6 and LPS used could induce TNF alpha, IL1 beta nor COX2 in foam cells over 2 hrs and 12 hrs of treatment. However, 2 hrs of IL6 (100 ng/ml) treatment in PMA-treated THP1 macrophages could only induce IL1 beta gene but not COX2 and TNF alpha (Figure 3a). Whereas LPS (500 ng/ml) could induce TNF alpha, IL1 beta and COX2 at 2 hrs of treatment but only IL1 beta at 12 hrs of treatment (Figure 3b).

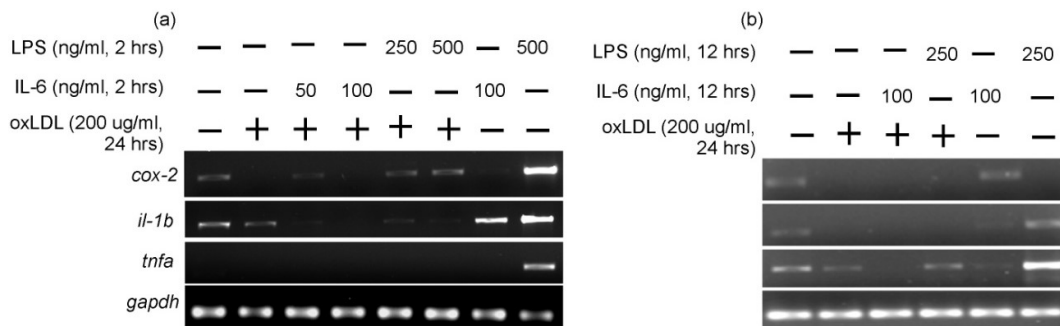


Figure 3: Gene expression profile of THP-1 derived foam cells. 3a. THP-1 macrophages were treated with 200 $\mu\text{g/ml}$ of oxLDL for 24 hrs followed by either IL-6 or LPS treatment for another 2 hrs. cox-2, il-1 β , tnf- α and gapdh gene expression was checked using semi-quantitative PCR. 3b. THP-1 macrophages were treated with 200 $\mu\text{g/ml}$ of oxLDL for 24 hrs followed by either IL-6 or LPS

treatment for another 12 hrs. *cox-2*, *il-1 β* , *tnf- α* and *gapdh* gene expression was checked using semi-quantitative PCR.

LDL is a very complex macromolecule which comprises of protein, triglycerides, cholesterol and phospholipids. LDL is uptaken by cells by LDL receptor (1). Oxidation of LDL produces an array of oxidized products (neo antigens) which are no longer recognized by LDL receptor. Precisely oxLDL is uptaken by scavenger receptors (CD36, SR-A, SR-B) in macrophages (2). Components of oxidized LDL, 9-HODE and 13-HODE activate Peroxisome proliferator-activated receptor gamma (PPAR γ) (3). PPAR γ in turns activates CD38 and downregulates NF-k β , STAT1 and AP-1 transcription factors (3, 4). Thus activation of PPAR γ leads to repression of pro-inflammatory cytokine production like IL1- β , TNF- α and macrophages primarily attain M2 phenotype (anti-inflammatory). In our experiment, ORO staining confirmed the formation of foam cells at 200 μ g/ml of oxLDL for 24 hrs of treatment. However, in foam cells, expression of pro-inflammatory cytokines was repressed as compared to THP1 macrophages. Treatment with IL6 as well as LPS for 2 hrs and 12 hrs could not induce expression of any pro-inflammatory cytokines genes tested over foam cells. *The reason for this could be that our treatment regime was unable to transform M2 (anti-inflammatory) foam cell to M1 (pro-inflammatory) macrophage.* With this understanding we had to change inducers for optimum induction of inflammation to elucidate any possible involvement of ribosomal proteins in inflammation-induced disease pathogenesis.

Inflammatory dose optimization of LPS, IL-6 and TNF- α for differentiated THP1 macrophages- Differentiated THP1 cells were treated with 10, 20, 50, 100 and 500 ng/ml of LPS, 10, 50 and 100 ng/ml of IL-6 and 10, 50 100 ng/ml of TNF- α for 2 hrs in 1% serum containing media. Cells were harvested with TRIzol for total RNA extraction.

LPS induced samples were checked for expression of *il-1 β* , *tnf- α* and *il-8* genes using semi quantitative PCR. *β -actin* served as endogenous control for all the samples. The lowest dose of LPS tested (10 ng/ml) could induce the expression of IL1 beta, TNF alpha and IL8 as compared reference sample (C) in 2 hr of treatment (Figure 4a). *il-1 β* and *tnf- α* which are early response genes of inflammation, increased in higher fold in compared to delayed response gene *il-8* in LPS treated samples in comparison to reference sample. Form the result; we have taken 100 ng/ml of LPS for optimum dose for induction of inflammation.

THP-1 macrophages were treated with 10, 50 and 100 ng/ml of human recombinant IL-6 for 2 hrs and *il-1 β* , *tnf- α* and *β -actin* mRNA abundance was checked using semi-quantitative PCR. Result showed that all the three concentrations of IL-6 could induce mRNA expression of *il-1 β* and *tnf- α* as compared to the untreated samples. However, we have chosen 50 ng/ml of IL-6 treatment for 2 hrs is optimum condition for inflammatory gene expression (Figure 4b).

il-1 β gene expression was checked for TNF- α induced inflammation in THP1 macrophages. Among the different doses of TNF- α used in this experiment, 10 ng/ml of TNF- α could induce highest level of *il-1 β* gene expression in 2 hrs of treatment. However, higher doses (50 and 100 ng/ml) of TNF- α could not induce *il-1 β* gene expression as compared to lowest dose

(10 ng/ml) of TNF- α (Figure 4c). So we have considered 10 ng/ml of TNF- α as optimum for induction of inflammation.

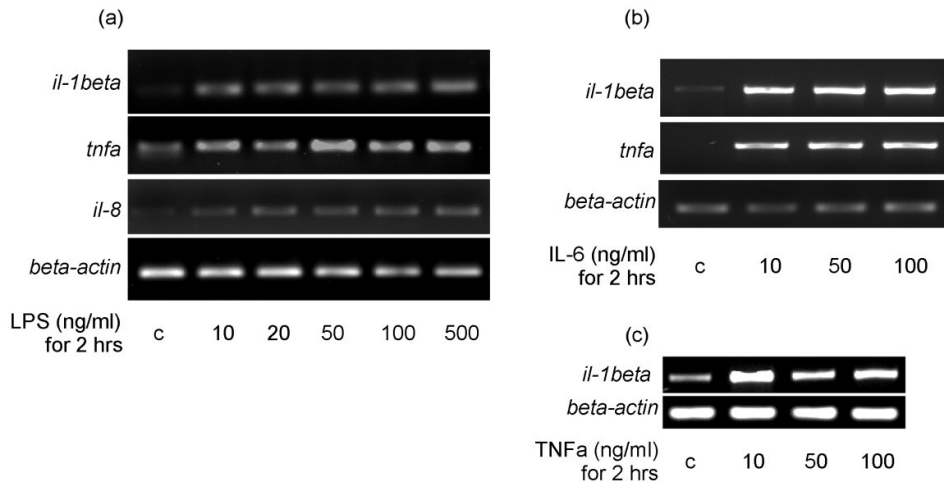


Figure 4: Inflammatory dose optimization of LPS, IL-6 and TNF- α for differentiated THP1 macrophages 4a. THP-1 macrophages were treated with varying concentration of LPS (10, 20, 50, 100 and 500 ng/ml) for 2 hrs. The expression of *il-1 β* , *tnf- α* , *il-8* and β -actin was checked using semi-quantitative PCR. 4b. THP-1 macrophages were treated with varying concentration of recombinant IL-6 (10, 50 and 100 ng/ml) for 2 hrs. The expression of *il-1 β* , *tnf- α* and β -actin mRNA was checked using semi-quantitative PCR. 4c. THP-1 macrophages were treated with varying concentration of recombinant TNF- α (10, 50 and 100 ng/ml) for 2 hrs. mRNA abundance of *il-1 β* and β -actin was checked using semi-quantitative PCR.

Microarray analysis- THP-1 macrophages were treated with optimized doses of 50 ng/ml of IL-6, 10 ng/ml of TNF- α and 100 ng/ml of LPS for 2 hrs (Figure 5a). Treatment was done in biological duplicates. Cells were then scraped using a cell-scraper and suspended in RNA Lateral (Ambion, USA). Total RNA was extracted using Qiagen RNeasy mini kit followed by DNaseI treatment. RNA concentration and quality was measured using nanodrop spectrophotometer and Bioanalyzer. Total RNA was labeled using T7 promoter based-linear amplification to generate labeled complementary RNA and hybridization was done using Agilent's in situ Hybridization kit on a Agilent's Human 8x15 Array. Microarray data was analyzed using GeneSpring GX Software (Agilent Technologies). The heat-map of the microarray data showed the overview of the expression pattern of all the 15 K genes used in the experiment. The heat-map also showed the high similarity of the pattern of gene expression between the biological duplicates (Figure 5b).

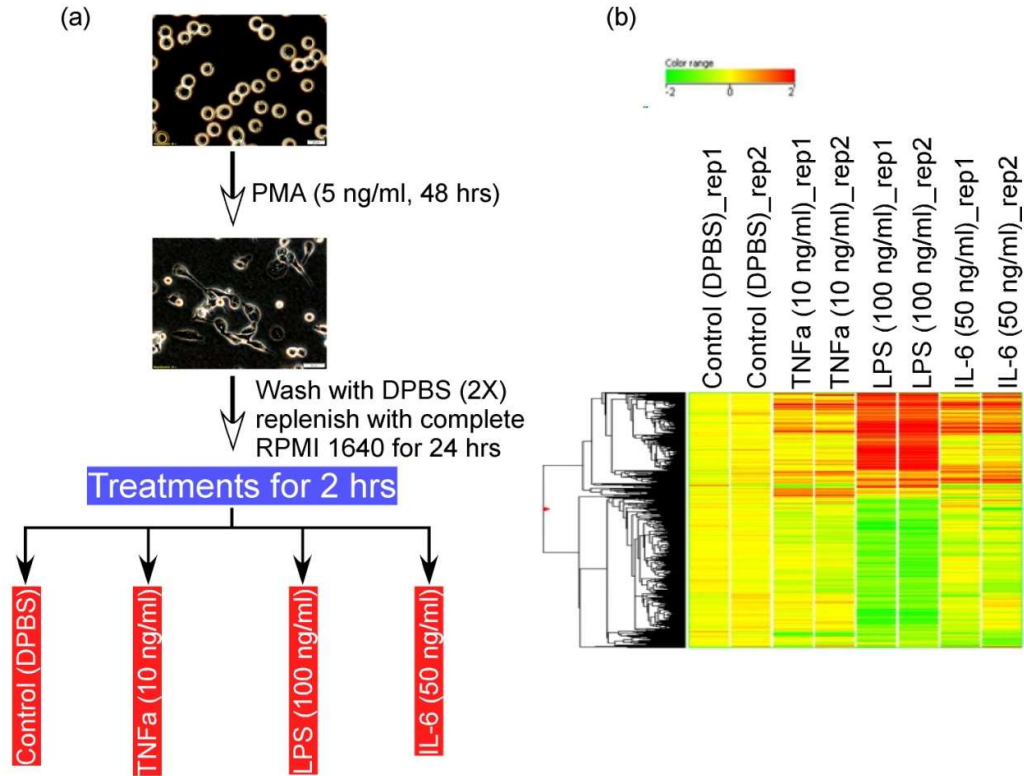


Figure 5: Microarray analysis. 5a. Schematic representation of treatment regime for microarray analysis. 5b. Heat map of 15k probes under TNF- α , LPS and IL-6 treatment in two biological replicates.

Microarray data validation- After critically analysis of the normalized microarray data we have identified 2.55 folds induction (**p=0.005) of a ribosomal protein, RPL22 in LPS (infective inflammation) induced THP-1 macrophages (Figure 6a, b). We have validated RPL22 gene expression in THP-1 macrophages treated with 100 ng/ml of LPS for 2 hrs using three different sets of human RPL22 gene specific exon junction primers using real time PCR (Figure 6c). Three different primers showed 1.91, 1.83 and 1.68 fold changes in respect to control untreated sample. This over-expression of RPL22 mRNA could significantly increase (4 fold) it's protein under LPS treatment as compared to the untreated cells (Figure 6d).

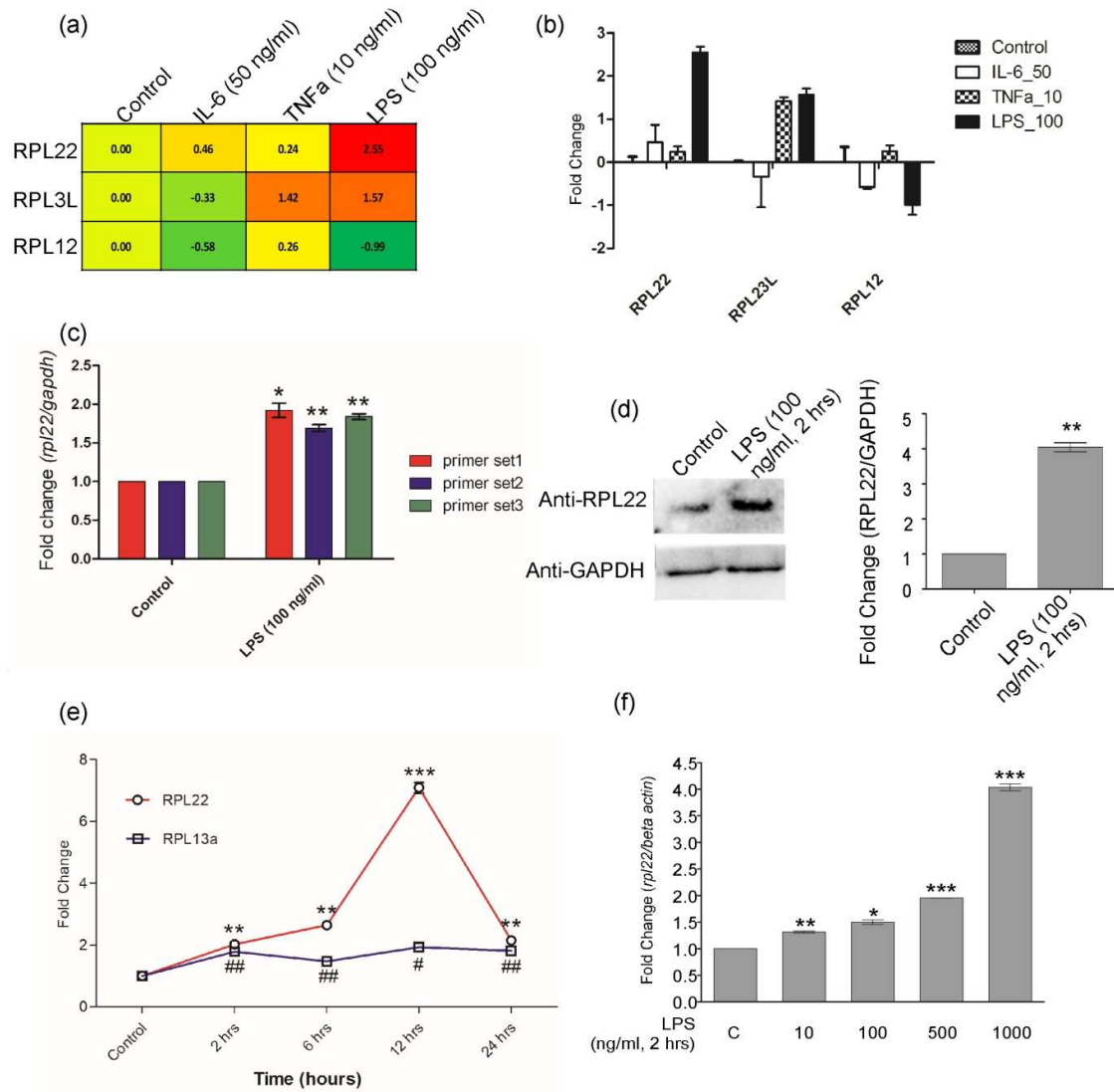


Figure 6: LPS-mediated inflammation up-regulated RPL22 expression. 6a and b. Gene expression profile of RPL22, RPL23L and RPL12 in three different treatment conditions that were IL-6, TNF- α and LPS at their respective concentrations. 6c. RPL22 gene expression was validated with three different sets of RPL22 exon junction primers using real time PCR. Two hours of LPS-treatment (100 ng/ml) significantly induced RPL22 gene expression in all the three sets of primers 6d. western blot analysis with anti-RPL22 showed that LPS-treatment (100 ng/ml) for 2 hrs significantly upregulated RPL22 protein expression as compared to the control cells. 6e. LPS time course study using real time PCR showed that RPL22 gene expression was robustly upregulated under LPS treatment as compared to the RPL13a. 6f. Real time PCR analysis showed that increasing concentration of LPS-treatment for 2 hrs also induced RPL22 gene in concentration dependent manner. Statistical analysis was performed by comparing treated samples with control sample by unpaired students' t-test using Graph pad prism (online version. ###/*** $p < 0.0005$, ##/** $p < 0.005$, #/* $p < 0.05$).

At this point we wanted to check how RPL22 gene expression changes over time under LPS treatment. We have treated the THP1 macrophages with LPS (5 ng/ml) for 0 hr, 2 hrs, 6 hrs, 12 hrs and 24 hrs. Real time PCR analysis showed that RPL22 gene expression increased from 0 hr over the time of treatment and became highest at 12 hrs (7.08 fold) and then went down to 2.15 fold at 24 hrs. However, another ribosomal protein RPL13a gene expression did not change over time of the treatment (Figure 6e). THP1 macrophage was treated with different concentration of LPS such as 10, 100, 500 and 1000 ng/ml for 2 hrs. RPL22 gene expression was checked using real time PCR. The gene expression of RPL22 increased linearly with the increasing concentration of LPS while another ribosomal protein gene RPS19 did not perturbed (Figure 6f). From these experiments we have concluded that LPS-mediated inflammation can specifically induce RPL22 gene.

Transcriptional up-regulation of RPL22 is NF- κ B dependent- To elucidate whether the increment of RPL22 mRNA and protein is because of transcriptional upregulation but not regulation at the post-transcriptional, we have analyzed promoters of RPL22 gene along with RPL2211, RPL13a, RPS19 and RPS11 in online server of MatInspector (5). Our analysis showed that RPL22 harbors four putative NF- κ B binding sites within 500 bp upstream of the transcription start site (TSS). While RPL2211, RPL13a, RPS19 and RPS11 genes possess one, none, two and one putative NF- κ B binding sites respectively within the span of the region (Figure 7a). We have cloned the 500 bp upstream sequence of RPL22 promoter into pGL3 basic plasmid (Figure 7b). The luciferase activity (RLU) of pGL3-rpl22 promoter vector was significantly higher in LPS treated and untreated MCF-7 cells as compared to the RLU from pGL3-basic vector transfected cells with similar treatment conditions. The treatment of Bay-11(a small molecule inhibitor of NF- κ B) followed by LPS significantly

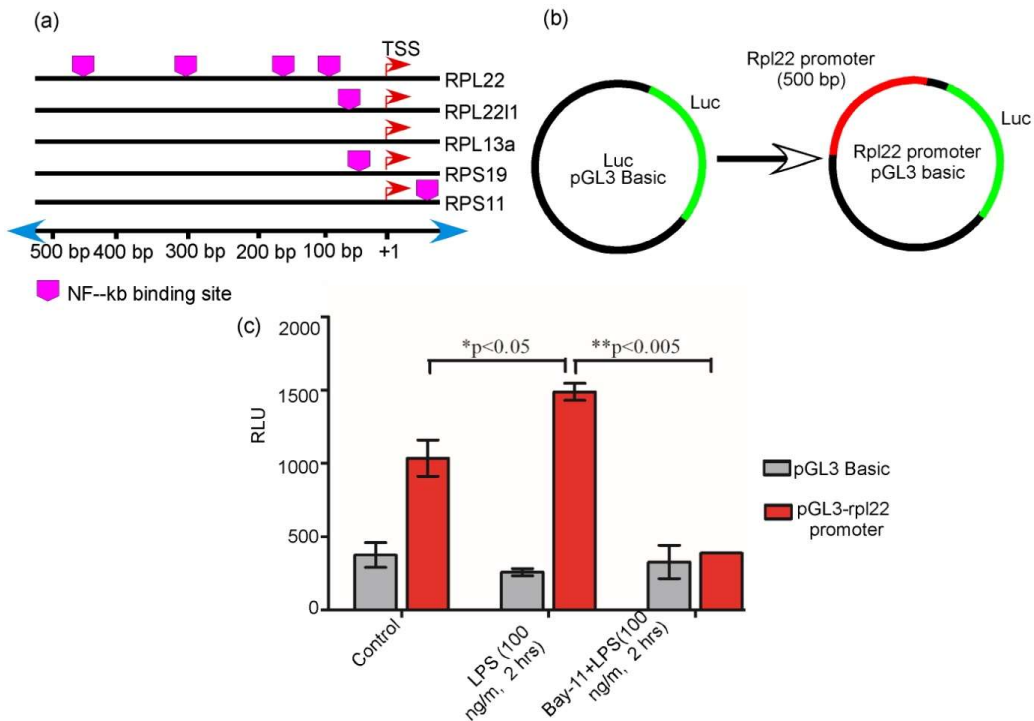


Figure 7: Transcriptional upregulation of RPL22 is NF- κ B mediated. 7a. *MatInspector* analysis showed that NF- κ B binding sites upstream of TSS of different ribosomal protein genes such as RPL22I1, RPL13a, RPS19, RPS11 along with RPL22. 7b. 500 bp up-stream of TSS of RPL22 gene harboring 4 putative NF- κ B binding sites was cloned into pGL3-basic vector. 7c. Luciferase reporter assay was performed in either pGL3-basic or pGL3-RPL22 promoter transfected MCF7 cells. Post-transfection cells were treated with either LPS or Bay-11 and LPS for 2 hrs. Statistical analysis was performed by unpaired students' t-test using *Gaph pad prism* (online version. ****p<0.005, *p<0.05**

reduced the luciferase activity in pGL3-rpl22 promoter plasmid transfected cells. These results suggested that the 500 bp promoter region of RPL22 gene was responsible for the transcriptional activation of the gene and NF- κ B may act as a transcription factor for LPS-mediated activation of RPL22 (Figure 7c).

Over-expression of RPL22 in THP-1 cells led to nuclear accumulation- To elucidate the sub-cellular location of over-produced RPL22 in a cell in LPS-mediated inflammation, we have performed immunofluorescence study. PMA differentiated THP-1 cells were either left untreated or treated with LPS (100 ng/ml) for 30 mins, 2 hrs and 6 hrs. Cells were washed twice with PBS and fixed in 4% paraformaldehyde and permeabilized in 1% TritonX100 containing PBS. Cells were then incubated with anti-RPL22 antibody. Cells were further washed with PBS for three times and incubated with anti-mouse secondary antibody tagged with Alexa Fluor 488. Cover-slips containing cells were mounted on the slides with Prolong Gold Antifade with DAPI (Invitrogen, USA). Images were taken in 100X in oil immersion using Olympus IX83 inverted fluorescent microscope (Olympus, Japan). Result showed that RPL22 present throughout the cell homogeneously in unstimulated cells whereas LPS-treatment induced RPL22 to be accumulated mostly in the nucleus. We found that 2 hrs LPS-treatment induced most profound accumulation of RPL22 in nucleus in respect to 30 mins and 6 hrs of the treatment (Figure 8b). To corroborate this finding, we have immunoblotted RPL22 of nuclear and cytoplasmic fractions of LPS-treated THP-1 cells at 0 hr, 30 mins, 2 hr and 6 hrs. Our result suggested that RPL22 was maximum enriched in nucleus at 2 hrs of LPS treatment. At 6 hrs of LPS treatment, RPL22 found to be more in cytoplasm than in nucleus as compared to 2 hrs of LPS treated cells in consistent with our immunofluorescence study (Figure 8a).

At this point we tried to understand whether nuclear accumulation of RPL22 is only restricted to LPS-mediated over-expression of RPL22, we have cloned RPL22 ORF into pBABEpuro plasmid and over-expressed the clone into THP-1 cells. Briefly, RPL22 ORF was amplified using RPL22 gene specific primer (reverse primer containing 6 poly-histidine codon) (Forward primer: 5'GCA TGA GGATCC GCC GCC GCC ATG GCT CCT GTG AAA AAG CTT GTG GTG 3', Reverse primer: 5'GCA TGA GAATTCTTA GTG GTG GTG GTG GTG ATC CTC GTC TTC CTC CTC TTC TTC3') from the cDNA sequence of THP-1 cells. Amplified product was then ligated into a TA vector (Invitrogen, USA) using T4 DNA ligase. The ligated product was then transformed into competent *E. coli* (DH5 α). The positive clones were screened using colony-PCR. The plasmids containing RPL22 CDS were isolated using QIAprep Spin Miniprep kit (Qiagen, USA). Isolated plasmid was double digested using BamH1 and EcoR1 restriction enzymes.

The empty pBABEpuro was also double digested using the same restriction enzymes. The double digested products of both the reactions were ligated (in 1:3 and 1:5 molar ratio) using T4 DNA ligase overnight. The ligated products were then competent E. coli (DH5 α) and grown in LB agar containing ampicilin plates overnight at 37°C. The positive colonies were screened using colony-PCR. The identified positive colony was further cultured in LB broth containing ampicilin and pBABEpuro-L22 CDS plasmids were isolated and DNA sequencing was performed for further confirmation.

Retroviral packaging: pBABE-puroL22 CDS (6.5 μ g), Gag-pol plasmid (5 μ g) and VSG-G plasmid (1 μ g) were mixed in 0.5 ml of RPMI 1640 (w/o serum & pen/strep) and incubate at RT for 5 mins. Separately 30 μ l lipofectamine 2000 (Invitrogen, USA) was added in 0.5 ml of RPLMI 1640 (w/o serum & pen/strep) and kept for 5 mins at RT. These two preparations were then mixed gently and incubated at RT for 30 mins. The mixture was then added drop-wise to the HEK293 cells (about 80% confluence) and allowed to transfect the cells for 8 hrs at 37°C incubator. After 8 hrs of incubation, the transfected cells were supplemented with fresh RPMI 1640 (with 10% FBS) media and incubated for another 24 hrs. The media containing retroviral particles was harvested and the cells were replenished with fresh media and incubated for another 24 hrs. The harvesting process was repeated for another two times. All the virus contaminating plastic-wares/glass-wares were decontaminated and discarded according to the institutional regulation.

Spinoculation of THP-1 monocytes: THP-1 cells (2.5 *10⁶) were added with 5 ml of virus containing RPMI media and 10 μ g/ml of polybrene and spun at 1000 g for 1 hr at RT in 15 ml falcon tube. The supernatant was discarded and infected cells were the incubated in RPMI 1640 with 10% FBS for 24 hrs. The spinoculation method was performed additional two times in 24 hrs intervals in new batches of virus particle containing RPMI 1640 media. After three stages of infection, cells were allowed to grow for two days in 10% FBS containing RPMI 1640 media. The positive cell population was selected in puromycin (1 μ g/ml) containing RPMI 1640 media.

Western blot and Immunofluorescence analysis: Wild type (WT) and RPL22 overexpressed THP-1 (OE) cells were harvested in RIPA buffer containing phosphatase and protease inhibitor and protein was isolated from whole cell lysate. Same amount of protein (15 μ g) was loaded in 15% SDS-PAGE for both the samples. Protein was blotted into PVDF membrane using semi-dry blotting system (TE 77 PWR, GE Healthcare, USA). The membranes were probed with anti-RPL22 and anti-His primary antibodies (Santa Cruz Biotechnologies, USA). After incubation with respective secondary antibodies, the blots were developed and imaging was performed in Chemi Doc XRS system (Biorad, USA). Both the blots showed higher expression of RPL22 protein in respect to WT cells (Figure 1B). GAPDH was used for loading control (Figure 8c).

WT and OE THP-1 cells were differentiated using PMA (using previously mentioned protocol). Cells were stained with anti-RPL22 antibody showed localization of RPL22 in nucleus while treated with LPS in both WT and OE THP-1 cells. OE cells also showed higher amount of immunofluorescence in comparison to WT cells. Anti-His antibody stained cells showed immunofluorescence in only OE cells confirming successful over-expression of His-tagged RPL22 in THP-1 cells. It also revealed a significant amount of nuclear localization of over-expressed RPL22 in both LPS treated and control OE THP-1 cells which further hints of a possible non-canonical function of RPL22 in inflammation (Figure 8d).

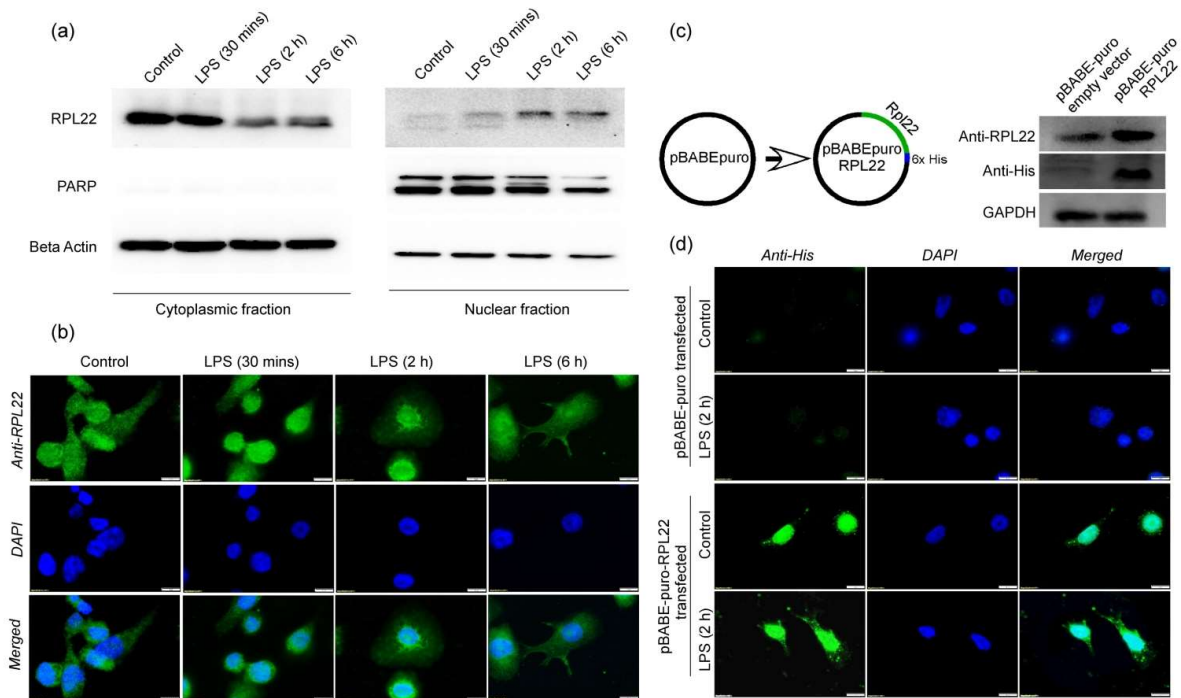


Figure 8: Over-expression of RPL22 in THP-1 cells led to nuclear accumulation. 8a. Nuclear-cytoplasmic fractions were made from LPS (100 ng/ml) treated THP-1 macrophages at 30 mins, 2 hrs and 6 hrs. The level of RPL22 was checked in these two fractions using anti-RPL22 antibody. 8b. Immunofluorescence study was done on LPS (100 ng/ml) treated cells at 30 mins, 2 hrs and 6 hrs using anti-RPL22 antibody. Pictures were taken using blue filter at 100X magnification (oil immersion). 8c. RPL22 ORF was cloned into pBABE-puro and over-expression of RPL22 was confirmed by immunoblot using anti-His and anti-RPL22 antibody. 8d. Immunofluorescence study was done on LPS (100 ng/ml) treated cells at 2 hrs using anti-His and anti-RPL22 antibody. Pictures were taken using blue filter at 100X magnification (oil immersion).

RPL22 binds to the 5' UTR of CCL2 mRNA -Recent studies on the extra-ribosomal functions of ribosomal proteins conceptualized the idea that many RPs can bind to the viral and cellular RNAs outside the context of ribosome. Some of the RPs such as human RPS13

(6) and yeast RPL30 (7), RPL32 (8) found to bind to their own transcripts and regulate the splicing. In addition to other extra-ribosomal functions of RPL22, it had been attributed to bind EBER1 (9, 10), telomerase RNA, and p53 mRNA (11). In this context, we hypothesized that the reason of selective over-expression of RPL22 in LPS-mediated inflammation is to regulate the inflammation through its RNA-binding capabilities. To get any clue to prove this hypothesis, cross link immunoprecipitation (CLIP) experiment was performed from LPS-treated and untreated THP-1 whole cell lysates and a series of genes involved in inflammation such as *tnf- α* , *il-6*, *ccl2*, *il-10*, *icam-1*, *vcam-1* and *il-1 β* were checked using RT-PCR (data not shown). The results from CLIP experiment revealed that only *ccl2* mRNA could interact with RPL22 in LPS-treated cells (Figure 9a). To justify the specificity of the interaction, we could not able to detect *ccl2* in sample pulled down with non-specific IgG or immunoprecipitated RNA samples without the reverse transcription (data not shown). We have only observed the RNA-protein interaction in LPS treated samples. This could be because of availability of more *ccl2* mRNA (as indicated in input samples) and RPL22 protein in LPS-treated THP-1 macrophages as compared to the LPS-untreated cells or there may be any post-translational modification of RPL22 by LPS-mediated inflammation responsible for its binding to the mRNA or RPL22 and *ccl2* mRNA do not share the same spatiotemporal entities. Nonetheless, at this point we were interested to check the cellular location of this RNA-protein interaction. THP-1 macrophages were treated with LPS for 2 hrs and nucleus and cytoplasm were separated out. The CLIP experiment, as described before was performed using anti-RPL22 antibody. Result showed that *ccl2* mRNA was enriched more in LPS-treated nuclear fractions as compared to the nuclear fractions of untreated cells and cytoplasmic fractions of LPS-treated and untreated cells (Figure 9b). This result was consistent with our previous observation on LPS-mediated nuclear accumulation of RPL22, which in turn facilitated the RNA-protein interaction in the nucleus under LPS-treatment.

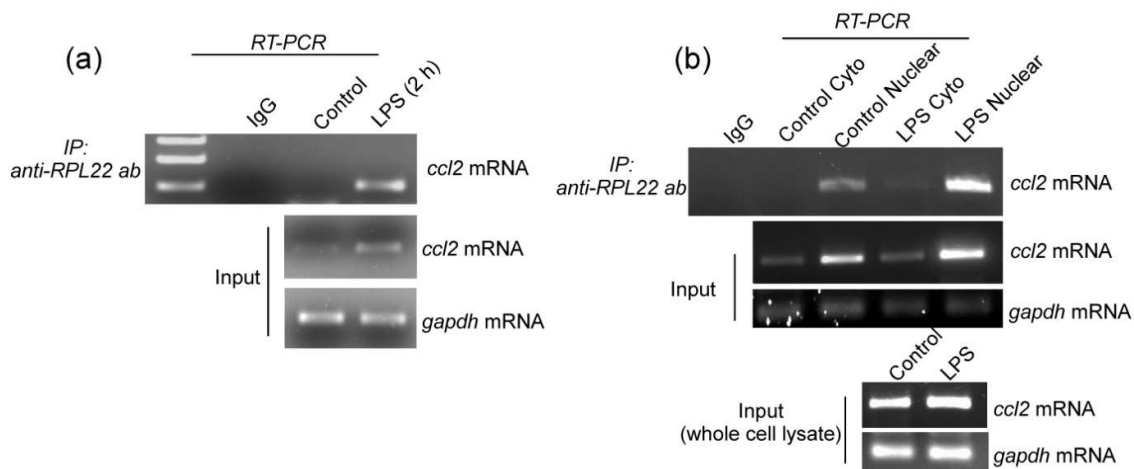


Figure 9: RPL22 binds to *ccl2* mRNA in nucleus in LPS-mediated inflammation. 9a. RNA-pulldown experiment was performed in LPS-treated (100 ng/ml) and untreated THP-1 macrophages with anti-RPL22 antibody conjugated with Sepharose protein 4G beads (invitrogen, USA). Eluted RNAs were checked using gene specific primers using semi-quantitative PCR. 9b. LPS-treated and untreated THP-1 macrophages were fractionated into nuclear and cytoplasmic parts according to the

manufacturer's protocol (NE-PER™ Nuclear and Cytoplasmic Extraction Reagents, Pierce, USA) and abundance of *ccl2* mRNA was checked in semi-quantitative PCR using *ccl2* gene specific primers.

As RPL22 was already been attributed for RNA binding protein, it was important to understand whether: a. RPL22 binds directly to the mRNA b. RPL22 binding site on the *ccl2* mRNA and c. nature of the interaction, we have performed *in vitro* RNA-protein binding assays. For this purpose, we have cloned human RPL22 ORF into pET32a bacterial expression vector to produce recombinant RPL22 protein for the experiments.

PCR amplification of RPL22 CDS from RPL22 cDNA sequence: THP-1 cDNA was used for the PCR amplification of RPL22 CDS using previously used primers and the PCR product was run on agarose gel. A single band against the 400 bp band on the ladder was observed in the lane containing the PCR product (Figure 10a)

Cloning of RPL22 CDS into TOPO TA cloning vector: To get precise double digested product, RPL22 CDS with Bam H1 and Eco R1 restriction enzyme sites was cloned into TOPO TA vector to get the double digested insert by restriction digestion after cloning. PCR amplification of RPL22 CDS was done using Taq polymerase which leaves an adenine at the 3' end of the product, creating overhangs or sticky ends. The TOPO TA vectors include 3'-thymine overhangs which aid in direct cloning of Taq-amplified PCR products. The PCR product and TOPO TA vector were mixed in the recommended buffer to facilitate their ligation.

The ligated product was transformed into DH5α *E. coli*. competent cells followed by spreading on LB agar plates containing ampicillin, IPTG and X-gal. White colonies were randomly selected for colony PCR. Colony PCR products were run on agarose gel for screening of cloned colonies. Colonies marked 1, 3, 4, 5 and 6 were successfully cloned (Figure 10b).

Double digestion of cloned TOPO TA vector and pET 32a vector: For sub-cloning RPL22 CDS into pET 32a (5900) vector, both pET32a and TA-RPL22 were digested with BamH1 and Eco R1 restriction enzymes. After digestion gel electrophoresis was performed. The double digested pET32a band was observed between 5000-7000bp (Figure 10d) and was excised out under an UV trans-illuminator. Similarly, the RPL22 CDS band observed between 400-500bp (Figure 10c) was excised out. Gel elution was performed for the excised bands.

Sub-cloning of RPL22 CDS into pET 32a vector: The double digested insert and pET 32a vector, after gel purification was ligated using T4 DNA ligase in T4 buffer system. The ligated product was transformed into DH5α *E. coli*. competent cells followed by spreading on LB agar plates containing ampicillin. 10 colonies were randomly selected for colony PCR. Colony PCR products were run on agarose gel for screening of cloned colonies. Colonies marked 2, 6 and 9 were successfully cloned (Figure 10e). Colony 6 was cultured and pET 32a-L22 plasmid was isolated. Isolated plasmids were double digested to re-confirm successful insertion of the insert and at last sent for sequencing to confirm the cloning. The alignment of the cloned sequences with the sequence available in the database was performed. The

alignment at the end is not matching as before the stop codon (TAA) 6 histidine codons (CAC) are present in the plasmid.

Protein expression and characterization: Colony 6 was cultured, and the isolated plasmid was transformed into competent BL21 DE3 *E. coli* cells. Recombinant protein was produced by IPTG mediated over-expression of cloned RPL22 CDS. The cells were then centrifuged and sonicated after re-suspending in bacterial lysis buffer. The cellular protein concentration in the bacterial cell lysate was quantified by Bradford assay and was separated by SDS PAGE. CBB staining showed significant over-expression (Figure 10f). The size of the recombinant protein was observed to be much greater than the original protein size (14.8 kDa) because of the presence of multiple tags in the plasmid between the promoter and cloned CDS which added about 20 kDa to the protein. This gave a final size below 37 kDa

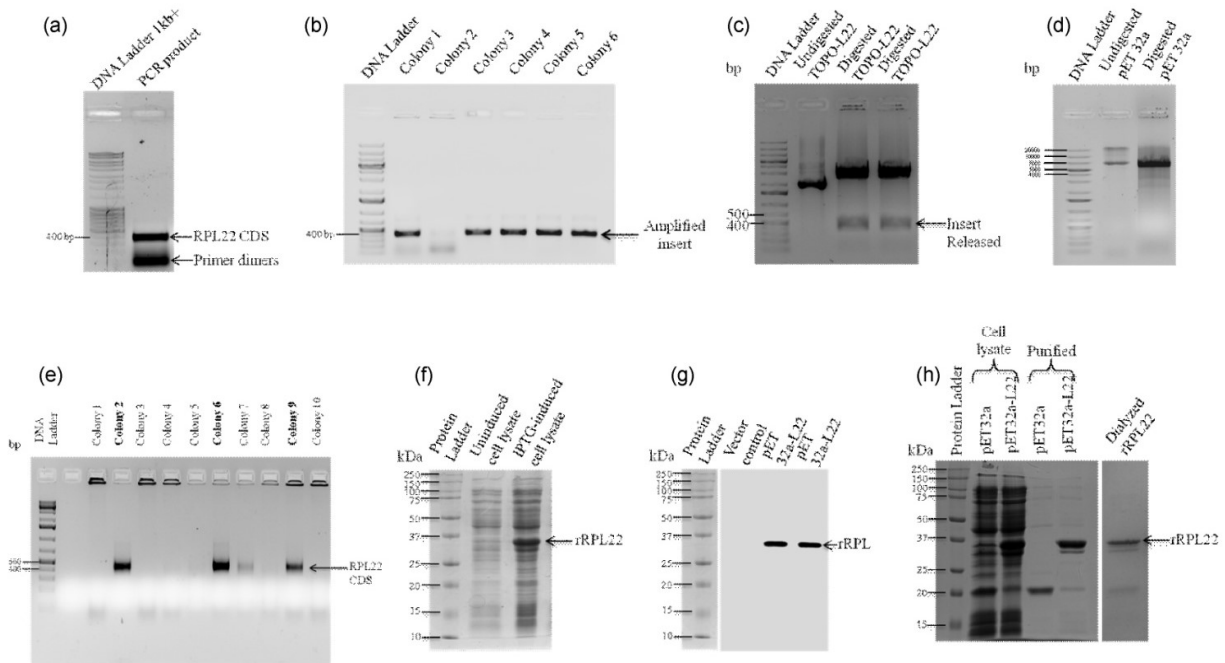


Figure 10: Cloning, characterization and purification of human recombinant RPL22. 10a. PCR amplified RPL22 ORF 10b. Colony PCR of RPL22 cloned in to pCR2.1-TOPO vector transformed into *E. coli* (DH5 α). 10c. Double digestion of pCR2.1-TOPO-RPL22 ORF with BamHI and EcoRI to release insert. 10d. Double digested pET32a vector with BamHI and EcoRI 10e. Colony PCR of pET32a-RPL22 ORF transformed into *E. coli* (DH5 α) 10f. Coomassie staining of SDS-PAGE of uninduced and IPTG-induced expression of recombinant RPL22 in *E. coli*-BL21 cells 10g. Immunoblot stained with anti-RPL22 antibody 10h. Coomassie staining of SDS-PAGE of Ni-NTA purified and dialyzed recombinant RPL22.

but much above 25 kDa when compared against the ladder as shown in Figure 10g. Western blot analysis with anti-RPL22 antibody confirmed over-expression and production of rRPL22 (Figure 10g).

Purification of recombinant RPL22: After characterization the bacterial cell lysate was purified by Ni-NTA purification method followed by dialysis to remove imidazole and other

salts used in the purification process. After both these steps Bradford Assay quantification, SDS PAGE and CBB staining was performed to confirm purification (Figure 10h).

UV-cross linking experiment

in vitro transcription: The T7 RNA polymerase templates for each of four fragments (5' UTR, ORF, 3' UTR and full-length mRNA) of *ccl2* mRNA were generated from cDNAs using Fusion DNA polymerase (NEB) using the following protocol and the primers.

PCR cycle was set for: Initial denaturation at 98°C for 2 mins, in cycle: denaturation at 98°C for 30 sec, annealing at 60 °C for 45 sec and polymerization at 72°C for 1min for 35 cycles, followed by final extension at 72 °C for 10 mins. The PCR products were run on the 1% agarose gel and purified using Qiagen gel-extraction kit. The purified templates were used for *in vitro* transcription:

Reagents	Amount (µl)
10X RNA transcription buffer	2
10 mM rATP	1
10 mM rGTP	1
10 mM rCTP	1
100 µM rUTP	1
αP ³² labeled UTP (Prit, Hyderabad)	2
Nuclease Free Water +Templates	10
100 mM DTT	1
T7 RNA pol	1

Samples were mixed well and incubated at 37°C for 1 hr for *in vitro* transcription.

Purification of the body labeled RNA: The probes were diluted using 180 µl of NFW and 3M sodium acetate (20 µl) was added to the 1/10th of the total volume. Glycogen (1 µl) and 400 µl of absolute alcohol were added to each samples and kept at -20 °C for overnight. The probes were spun at 13k RPM for 20 mins at 4°C. The supernatant was discarded from the opposite side of the pellet and washed with 70% alcohol at 13K rpm for 10 mins at 4°C. The pellets were air dried and reconstituted in 20 µl NFW. The radioactivity count was taken in H3 chamber (Liquid scintillation chamber, Hidex). Same amount of cpm count per length were taken for each probes.

Binding pf RPL22 with RNA:

- i. **6X binding buffer** = 2 µl
- ii. **10 µg/µl tRNA (yeast tRNA, Sigma, Cat No R8759)** = 1 µl
- iii. **RNase Inhibitor** =0.25 µl
- iv. **Nuclease free water** =as required

	5'UTR				ORF				3'UTR				Full length			
	C	BSA	L22 (200 ng)	L22 (400 ng)	C	BSA	L22 (200 ng)	L22 (400 ng)	C	BSA	L22 (200 ng)	L22 (400 ng)	C	BSA	L22 (200 ng)	L22 (400 ng)
Master mix	4	4	4	4	4	4	4	4	4	4	4	4	4	4	4	4
NFW	4.3	3.3	3.3	2.3	4.4	3.4	3.4	2.4	2	1	1	-	3.6	2.6	2.6	1.6
rRPL22	-	1	1	2	-	1	1	2	-	1	1	2	-	1	1	2
Probe*	0.7	0.7	0.7	0.7	0.6	0.6	0.6	0.6	3	3	3	3	1.4	1.4	1.4	1.4

*1,00,000 cpm count per fragment was taken

The experiments with radioactivity (UV-Crosslinking assay) was performed in the laboratory of **Dr. P. S. Ray, IISER-Kolkata.**

UV cross-linking experiment suggested that RPL22 binds only to 5'UTR mRNA in a concentration dependent manner (Figure 11a). To justify the specificity of the binding we have taken bovine serum albumin (BSA) as control protein and equivalent amount (100000 cpm/length) of probes were taken for each mRNA fragments. To understand the nature of RNA that binds to the RPL22, we have equal amount of radio labeled 5'UTR and folded in three different ways: one was kept as it attained the structure rendered by T7 RNA polymerase, second probe was heated to 95 °C and then snap freeze to linearize and the third one was heated to 95 °C followed by gradual decrease to room temperature so that it can attain minimum energy structure. With these three kinds of probes, the binding study of RPL22 showed that RPL22 can bind maximum to the linear structure of 5'UTR (Figure11b) suggesting a sequence dependent RNA protein interaction.

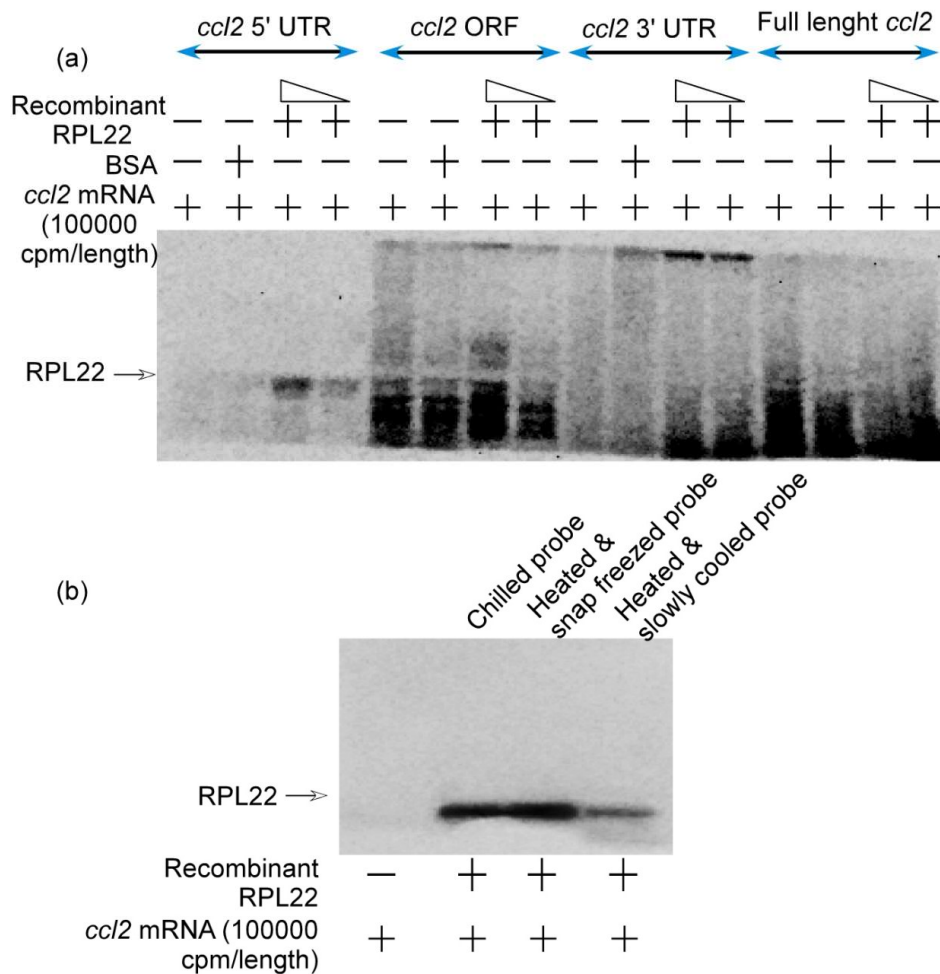


Figure 11: RPL22 binds to *ccl2* mRNA on its 5' UTR *in vitro*. 11a. Auto-radiogram showing the binding of recombinant RPL22 with 4 varying parts of *ccl2* mRNA separately namely 5' UTR, ORF, 3' UTR and full length mRNA. Result showed that rRPL22 can bind to the 5' UTR of *ccl2* mRNA. 11b. The probe for 5' UTR of *ccl2* mRNA was prepared with 3 different ways such as chilled probe, heated and snap frozen probe and heated and slowly cooled probe and allowed to bind to RPL22 protein. Heated and snap frozen probe showed highest binding to RPL22 hinting that this RNA-protein interaction is sequence dependent.

Characterization of RPL22-*ccl2* mRNA binding by Isothermal Titration Calorimetry:

Recombinant RPL22 and *in vitro* transcribed *ccl2* mRNA fragments were sent for isothermal titration calorimetry at DBT-CU-IPLS core facility, University of Calcutta. The binding isotherms and thermograms of the titrations were received (Figure 12) and used for calculating other parameters (Table 1). All the information was used for interpretation of the data and drawing out meaningful conclusions about the *in vitro* binding characteristics of rRPL22 and *ccl2* mRNA fragments.

<i>ccl2</i> mRNA	5' UTR		CDS	3' UTR		Full length	
ka	243000.0	216000.0	797000.0	241000.0	247000.0	172000.0	144000.0
ΔG	-7.6	-7.6	-8.4	-7.6	-7.7	-7.4	-7.3
ΔH	-5483.0	-498700.0	-9687.0	-6415.0	-1304000.0	-20900.0	-301300.0
TAS	-5475.4	-498692.4	-9678.6	-6407.4	-1303992.3	-20892.6	-301292.7
ΔS	-17.7	-1610.0	-31.2	-20.7	-4210.0	-67.4	-972.0
Binding Model	Sequential Binding Sites		Single Site	Sequential Binding Sites		Sequential Binding Sites	

Table 1: ITC generated and calculated thermodynamic values along with proposed binding model for rRPL22 titrated against different *ccl2* mRNA fragments.

The ITC experiments were carried out at a molar ratio of 1:40 :: titrand (RNA) : titrant (rRPL22) at 37°C. All the titrands showed a significant positive association constant (k_a) and a very high negative change in enthalpy (ΔH) upon titration with rRPL22. In general, a very high negative ΔH is considered a characteristic of H-bonding and/or van der Waal's interactions (12). The first ΔH upon titration of full length *ccl2* mRNA with rRPL22 was approximately equal to the sum of first ΔH of the individual fragments. Gibbs free energy (ΔG) for the full length as well as all the individual fragments of *ccl2* mRNA was negative. Binding of rRPL22 with CDS of *ccl2* mRNA had the highest thermodynamic favorability as a more negative ΔG indicates tighter binding (13). A negative change in entropy (ΔS) suggests increase in the order of the system, post binding. Hence, binding of rRPL22 *in vitro* might be leading to a more stable secondary structure of the RNA fragments. Since both ΔH and ΔS (change in entropy) were negative, the thermodynamic favorability of the reactions depended significantly on the temperature. All ITC titrations were enthalpy driven (12) i.e. a very exothermic reaction overcame a decrease in entropy giving a negative ΔG at 37°C. *in vitro* binding characteristics of rRPL22 to different fragments of *ccl2* mRNA using ITC suggested strong binding of rRPL22 with all the fragments. Sequential binding site model was proposed for the full length RNA along with the 5' and 3' UTR RNA fragments while the CDS RNA fragment which also had the strongest binding was best fit into the single site binding model. Also, the binding of the recombinant RPL22 with the mRNA fragments could be via H-bonding or van der Waal's interactions and might be either stabilizing the secondary structure of the RNA or converting the same into a structure having higher stability.

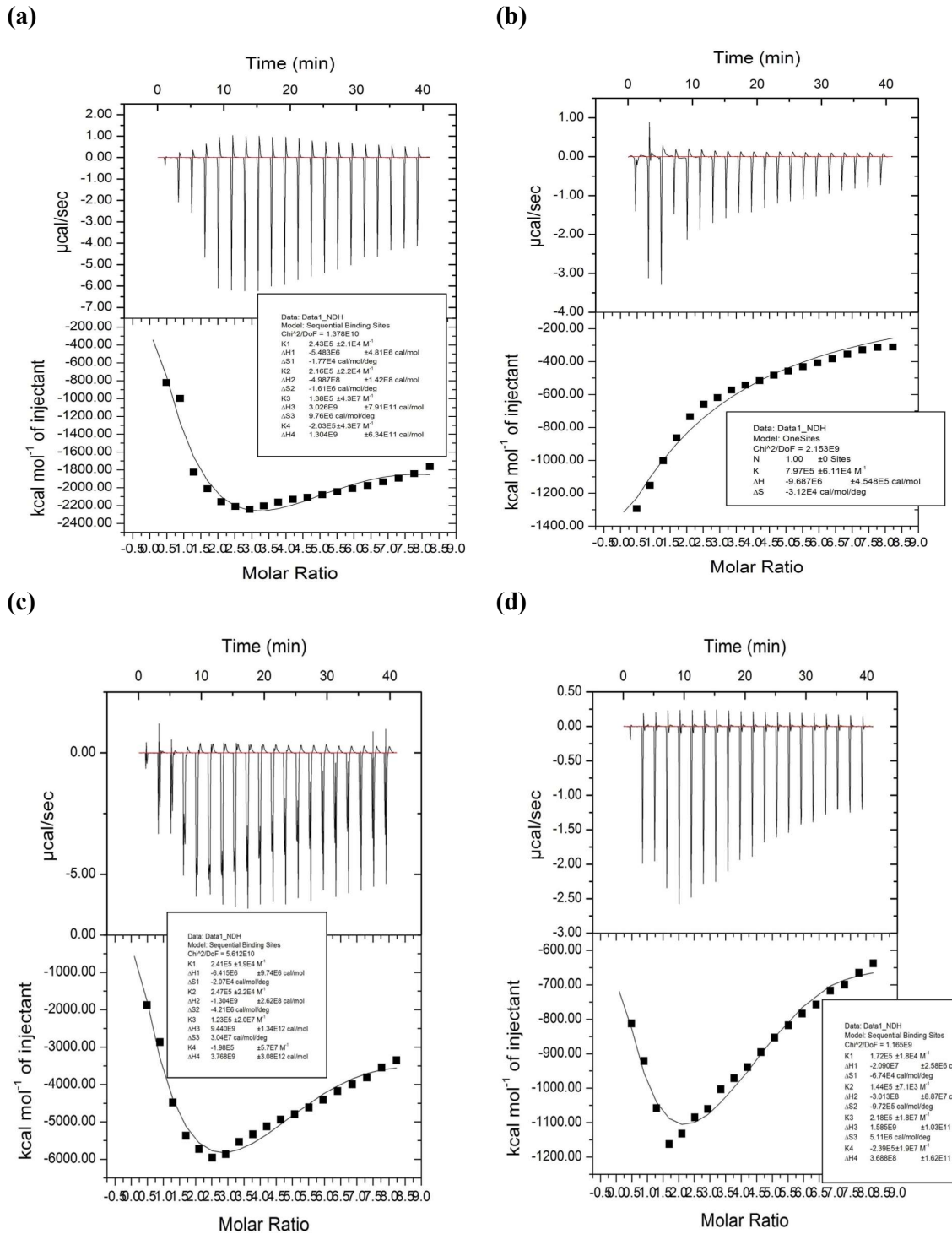


Figure 12: Thermogram (above) and binding isotherm (below) of recombinant RPL22 protein titrated against (a) 5' UTR, (b) CDS, (c) 3' UTR and (d) full length *cc12* mRNA. Data fits best in sequential binding site model.

Knockdown of RPL22 augments CCL2 expression- To understand the functional link between *ccl2* and RPL22, we have checked the *ccl2* mRNA and cellular protein level in THP-1 macrophages treated with either RPL22 siRNA or scrambled siRNA (Figure 13a). Our result revealed that siRNA-mediated knock down of RPL22, significantly up-regulated the *ccl2* mRNA and protein expression. The treatment of LPS for 2 hrs in RPL22 knocked down cells further augmented the *ccl2* mRNA as its protein expression (Figure 13 b, c, d).

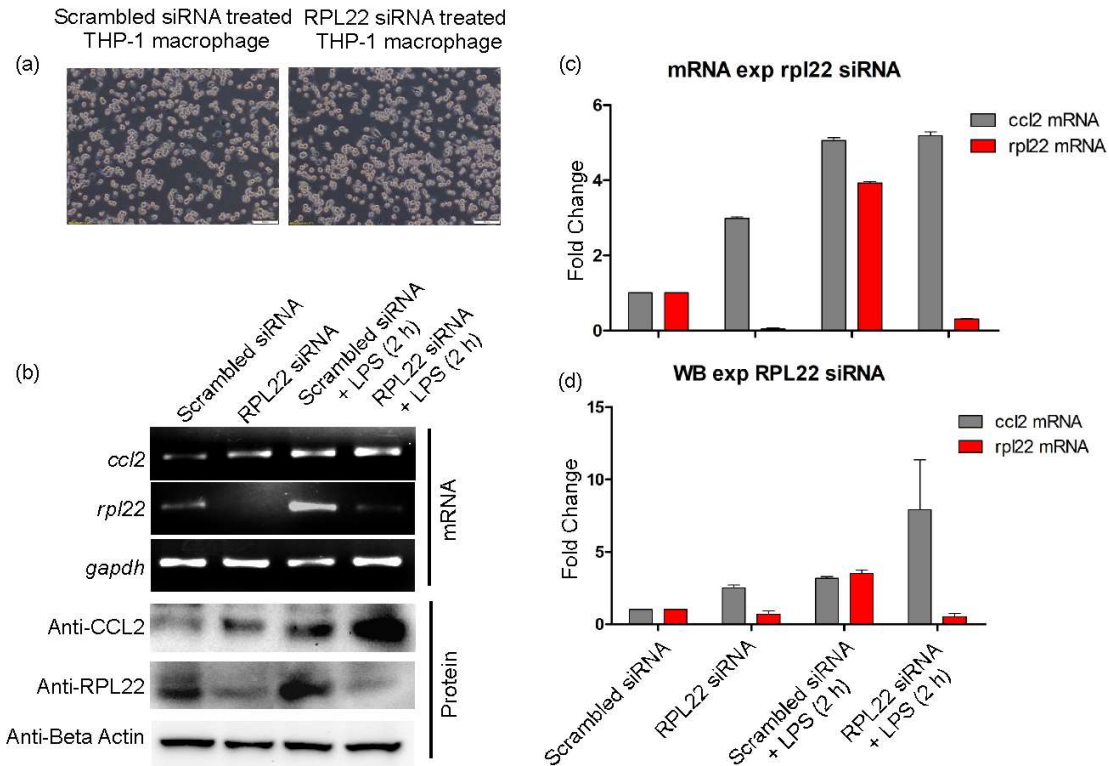


Figure 13: Knock down of RPL22 up-regulates *ccl2* mRNA and protein expression. 13a. Phase contrast cell micrograph of THP-1 macrophage cells treated with either scrambled siRNA or RPL22 siRNA (10X magnification), showing no apparent morphological abnormality. 13b. Semi-quantitative PCR and western blot were performed in scrambled siRNA or RPL22 siRNA treated THP-1 cells. Post-transfection cells were treated with LPS (100 ng/ml) for 2 hrs. CCL2 and RPL22 mRNA and protein expression was checked. 13c. Densitometric analysis was performed on *ccl2* and *rpl22* mRNA expression profile of siRNA treated samples. 13d. Densitometric analysis was performed on CCL2 and RPL22 protein expression profile of siRNA treated samples.

To confirm the effect of RPL22 on *ccl2* production, we have knocked out (KO) RPL22 in MCF7 cells by CRISPR-Cas9 method.

Generation of RPL22 KO MCF7 cell line

Construction of guide RNA (gRNA) against human RPL22 gene: Two sets of gRNA were constructed using www.benchling.com against RPL22 exon 1 (Figure 14a).

Cloning of RPL22 gRNAs into pSpCas9n(BB)-2A-puro V2: gRNA-forward and gRNA-reverse oligos were resuspended in TE buffer to 100 μ M concentration. 1 μ l of each oligos were combined with 1 μ l of T4 ligation buffer (10X), 0.5 μ l T4 PNK and 6.5 μ l of ddH₂O for a 10 μ l total reaction. The oligos were reannealed using the following protocol: 37 °C for 30 mins, 95 °C for 5 mins, ramp down to 25 °C at 5 °C/ min. The annealed oligos were diluted (10 μ l) by adding 90 μ l of dddH₂O. pSpCas9n(BB)-2A-purov2 (Addgene) vector was digested using the following protocol: 1 μ g of pSpCas9n(BB) was combined with 1 μ l of BbsI, 1 μ l of FastAP, 2 μ l of 2X FastDigest buffer X μ l of ddH₂O to a final volume of 20 μ l and incubated for 30 mins at 37°C. The digested vector was purified by gel extraction. The digested vector and reannealed oligos were then ligated using the following protocol: 50 ng of digested vector was combined with 1 μ l annealed oligo complex, 5 μ l of 2X Quick ligation buffer, 1 μ l of Quick ligase and X μ l of ddH₂O to 11 μ l total reaction mixture and incubated at 37° C for 15 mins. Competent E coli (DH5 α) (100 μ l) was transformed with 2 μ l of ligated reaction mix. Positive colonies were identified using colony PCR. Selected positive colonies for each gRNA were grown in LB broth and cloned plasmids were isolated (Figure 14b).

Transfection into MCF-7 cells and selection of positive cells: A 500 ng of total plasmid was transfected using Lipofectamine 2000 according to the manufacturer’s protocol. Following 72 hrs of the transfection, the vector control as well as gRNA positive cells were selected with 1 μ g/ml of puromycin for another 3 days. The dead-negative cells were washed with PBS and the positive cells were replenished with fresh complete DMEM.

Clonal selection: After the puromycin selection, a total of 60 cells were seeded in a 96-well plate such a way that each well contain single cell and let it grow up to confluence. Clones from each well were harvested and genomic DNA was isolated. A replica plate was made to

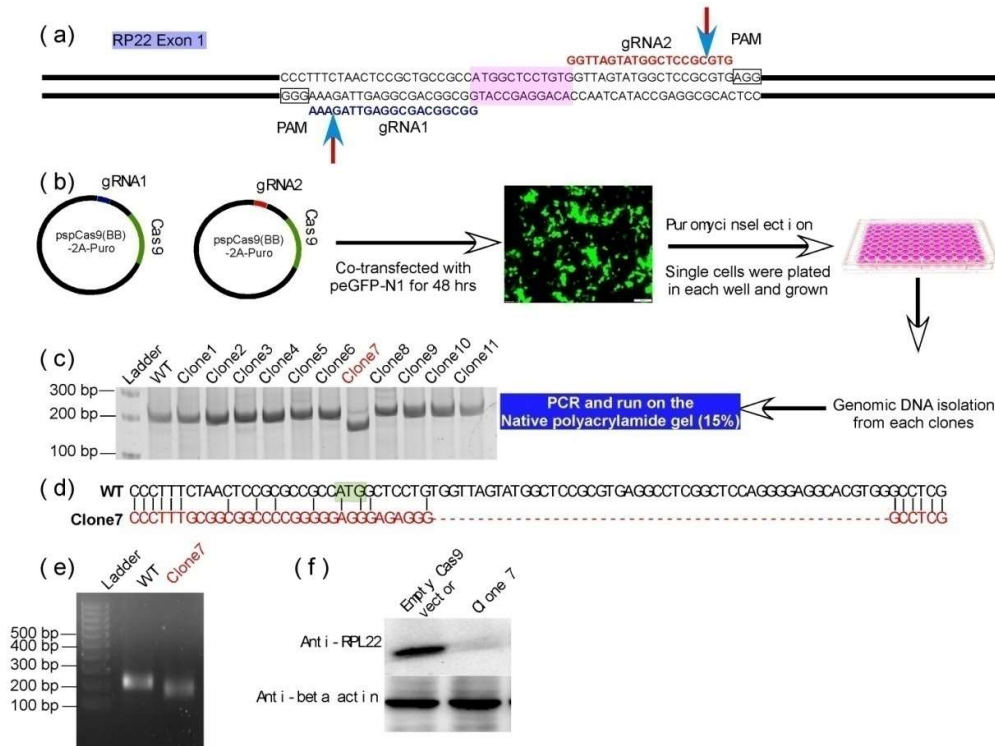


Figure 14: CRISPR-Cas9 mediated knock out of RPL22 from MCF7 cells. 14a. paired guide RNAs were designed against first exon of RPL22 gene. 14b. Two gRNAs were cloned into spCas9(BB)-2A-Puro vector and co-transfected to MCF7 cells with pEGFPN1 vector. The positive transfected cells were selected through puromycin selection for 3 days. The positive transfected cells were singularly grown in 96-well plate and genomic DNA was isolated. The target site was amplified with a flanking set of primer and run on native polyacrylamide gel (15%) in 0.5XTBE buffer. 14c. Among the screen clones, clone7 showed expected deletion. 14d. the CRISPR-Cas9 mediated deletion was further confirmed DNA sequencing 14e. The deletion was run on agarose gel in TAE buffer. 14f. The knock out of the RPL22 gene was validated by western blotting against anti-RPL22 antibody.

each of the single clones. The target sequence of RPL22 Exon1 was amplified using flanking primers in a semi-quantitative PCR. The PCR product was then run on 15% polyacrylamide native gel in 0.5X TBE running buffer. After the run, gel was washed with ddH₂O and stained with Sybr Green and visualized in ChemiDoc XRS system (Biorad, USA). The clone with deletion was identified (clone 7, Figure 14c) and subjected to further confirmation of CRISPR-Cas9 mediated deletion by DNA sequencing. The successful KO of RPL22 from MCF7 cells were further confirmed by western blotting against anti-RPL22 antibody (Figure 14f).

RPL22 knock out cells did not show any phenotypic changes under the phase contrast microscope as compared to the RPL22 WT MCF7 cells (Figure 15a). Although the growth rate of RPL22 KO cells were significantly higher than the RPL22 WT cells (Figure 15b), the level of pre-45S rRNA did not change in KO cells, suggesting an unaltered ribosome biogenesis in absence of RPL22 (Figure 15c). The knocking out of RPL22 induced the *ccl2* at mRNA and protein level as compared to the RPL22 wild type cells, while LPS treatment for 2 hrs on KO cells could induce further *ccl2* mRNA but not in protein level like the knocked down cells (Figure 15d,e,f). We have also checked the CCL2 protein level in RPL22 KO and wild type MCF-7 cells in 1 hr, 2 hr, 4 hr, 6 hr and 8 hr of LPS challenges by western blot. The result revealed that *ccl2* protein was induced in LPS treatments as compared to untreated cells and highest induction was observed at 4 hr of the treatment followed by diminishing of the protein level in subsequent hours in RPL22 wild type cells. Whereas LPS-untreated RPL22 KO cells showed a heightened level of CCL2 protein (fold change 3.2) as compared to the untreated RPL22 WT although we have loaded same amount whole cell lysate (25 µg). LPS treatment for following hours (1 hr, 2 hr, 4 hr, 6 hr and 8 hrs) on RPL22 KO cells did not show any significant induction as compared to the untreated RPL22 KO cells. These result suggested that the loss of RPL22 puts cells to continuous production of CCL2 (Figure 15 g,h).

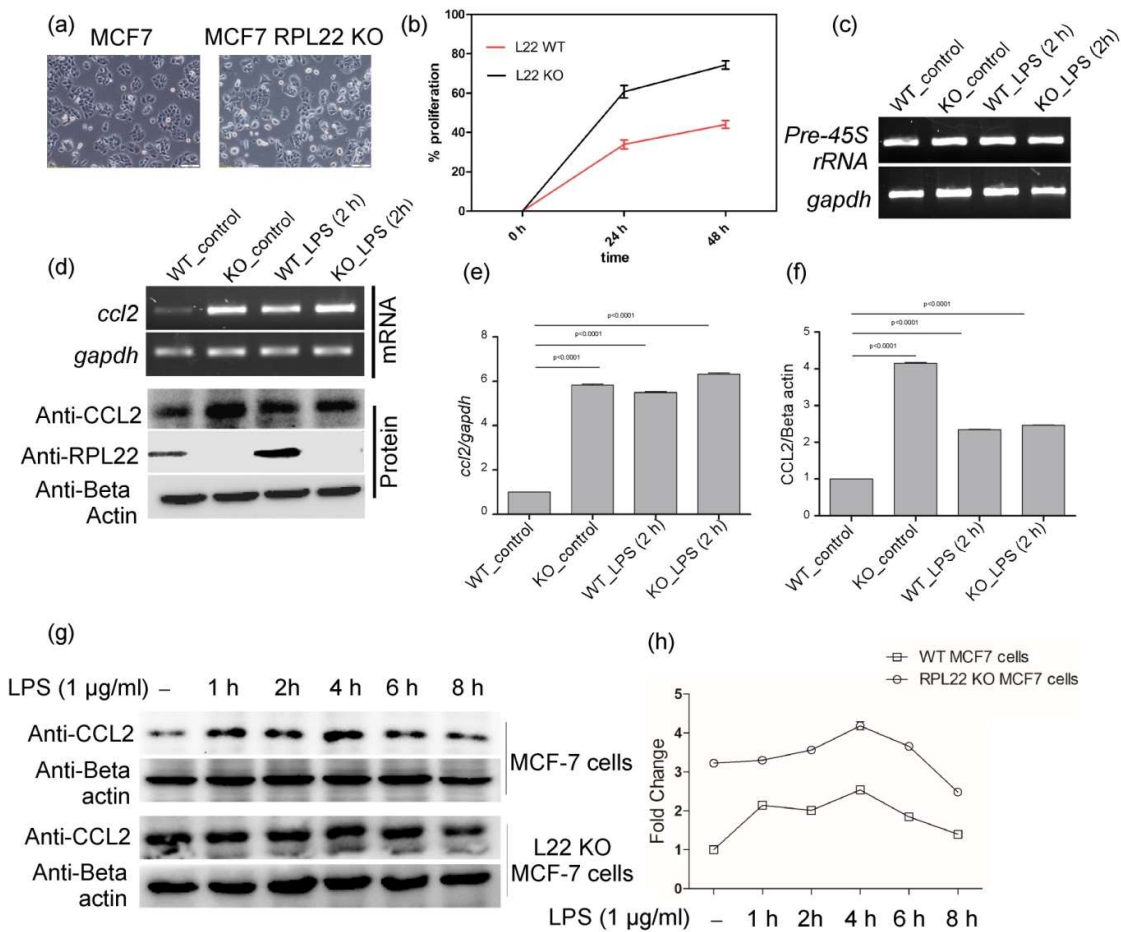


Figure 15: RPL22 knock out induced *ccl2* mRNA and protein expression in MCF7 cells. 15a. RPL22 knock out cells did not show any phenotypic changes under the phase contrast microscope as compared to the RPL22 WT MCF7 cells. 15b. Proliferation rate of RPL22 KO and WT cells was checked using MTT assay. 15c. Semi-quantitative PCR analysis of pre-45S rRNA showed no change in ribosome biogenesis. 15d. Semi-quantitative PCR and western blot analysis *ccl2* mRNA and protein in RPL22 KO and WT MCF7 cells. 15e, f. Densitometric analysis of *ccl2* mRNA and protein expression from semi-qRT PCR and western blot data. 15g. Western blot analysis of *ccl2* in time dependent LPS treated RPL22 KO and WT MCF cells. 15h. Densitometric analysis of *ccl2* western blot data from LPS time dependent study.

RPL22 degrades *ccl2* mRNA by binding to its 5'UTR- To investigate the biological significance of RPL22 binding to the 5'UTR of *ccl2* mRNA, we have performed mRNA degradation assay in RPL22 wildtype and KO MCF7 cells. RPL22 KO MCF7 and WT MCF7 cells were treated with LPS (1 µg/ml) for 2 hrs prior to 5 µg/ml Actinomycin D (Sigma, USA) for indicated time periods (14). Cells were harvested and total RNA was isolated using Aurum total RNA mini kit (Biorad, USA). The amount of *ccl2* mRNA in each samples were checked using gene specific primers in semi-quantitative PCR. (Figure 16a). RT-PCR analysis using *ccl2* gene specific primers revealed that in genomic deletion of RPL22 increased the half-life of *ccl2* mRNA up to 8 hrs of transcription inactivation as compared to the RPL22 wild type cells where the *ccl2* mRNA degradation was significantly rapid (Figure 16b). The deletion of RPL22 led to the 72.76% accumulation of initial *ccl2* mRNA at 8 hrs of

Act D-mediated transcription inactivation while in WT cells it was only 7.5% of initial *ccl2* mRNA that remained at 8 hrs of Act D treatment.

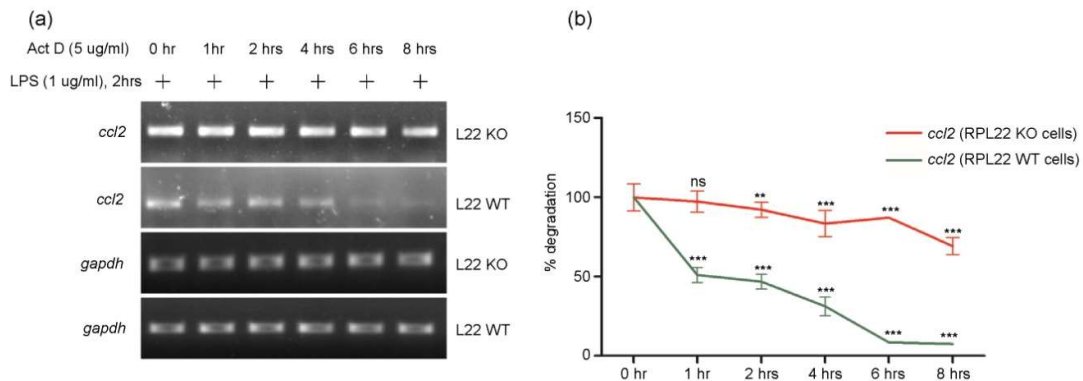


Figure 16: RPL22 degrades *ccl2* mRNA by binding to its 5'UTR. 16a. *ccl2* mRNA degradation assay semi-quantitative PCR analysis of in RPL22 KO and WT MCF7 cells. 16b. Densitometric analysis of *ccl2* mRNA turn over in RPL22 KO and WT MCF7 cells. Statistical analysis was performed by comparing treated samples with control sample by unpaired students' t-test using Gaph pad prism (online version). *** $p < 0.0005$, ** $p < 0.005$, * $p < 0.05$.

To further confirm the role of RPL22 binding to the *ccl2* 5'UTR, we have cloned the 5'UTR in between the SV40 promoter and Fluc ORF in pGL3-promoter vector.

Cloning of *ccl2* 5'UTR into PCR2.1-TOPO vector: *ccl2* 5'UTR was amplified from cDNA using DynazymeTaq DNA polymerase and cloned into PCR2.1-TOPO vector and positive white colonies (Blue-White screening) was identified using colony PCR. Plasmid DNA was isolated using HiPurA plasmid DNA isolation kit (Himedia) and the insert was released by double digestion using HindIII and NcoI.

Sub-cloning of *ccl2* 5' UTR into pGL3 promoter vector: The pGL3 promoter vector was double digested using HindIII and NcoI and ligated with double digested insert in molar ratio of vector:insert = 1:10. The ligated vectors were the transformed into competent DH5 α E. coli cells and spread on LB plates containing 100 μ g/ml Ampicilin containing plates. The positive clones were then identified using colony PCR and plasmids were then isolated HiPurA plasmid DNA isolation kit (Himedia). The positive clone was affirmed by PCR against *ccl2* 5'UTR specific primers and sequencing.

All the vector preparations as depicted in Figure 17a were transfected in MCF7 cells and LPS (1 μ g/ml) treatment was done for 2 hrs after 48 hrs post transfection. Luciferase activity assay showed that LPS-treatment did not have any effect on empty pGL3-promoter transfected cells as compared to the LPS-untreated counterparts. Interestingly, when cells were introduced with 5'UTR harboring pGL3-promoter vector, it showed significantly lower luciferase activity in both LPS-treated and untreated cells as compared to the cells were introduced with empty plasmid. In previous studies we have seen that LPS-treatment induced RPL22 and it is well established fact that LPS robustly induce *ccl2* mRNA (15, 16). At this point we speculated that LPS treatment might have effect on luciferase activity of 5'UTR containing plasmid by

any other RNA binding protein except RPL22. To understand the specific role of RPL22 on 5' UTR binding, we have over-expressed RPL22 in MCF7 cells and followed by transfection LPS-treatment was performed. Result showed that luciferase activity was significantly diminished in LPS-treated RPL22 over-expressed cells as compared to the LPS-treated WT cells. But RPL22 over-expressed MCF7 cells did not show any significant change in luciferase activity as reference to the WT cells. This may be because of only RPL22 binding does not degrade the message, possibly indicating to the involvement of other proteins that require for the RPL22 mediated degradation (Figure 17b).

As we have introduced the 5'UTR between the SV40 promoter and FLuc ORF without disturbing the reading frame (Figure 17a), we wanted to confirm that significant change of luciferase activity was only due to the less stability of mRNA itself, not because of the anomaly in translation of luciferase. To address this question, we have co-transfected MCF7 cells either with empty pGL3-promoter or pGL3-5'UTR and pSV-β-galactosidase plasmids and treated with LPS (1 μg/ml) for 2 and 6 hrs. RT-PCR analysis using specific primers for

FLuc gene showed that LPS treatment on pGL3-5'UTR transfected cells significantly diminished the FLuc mRNA at 6 hrs (0.5 fold) as compared to the LPS-untreated cells (Figure 17c, d). The level of FLuc mRNA was unaltered across the LPS-treatment on pGL3-promoter transfected cells. The level of β-galactosidase mRNA was even across the samples, suggested that decrease of FLuc mRNA was not due to the difference in transfection efficiency among the samples. These results revealed that down regulation of luciferase activity in pGL3-5'UTR transfected cells upon RPL22 over-expression is not due to defective translation of luciferase enzyme.

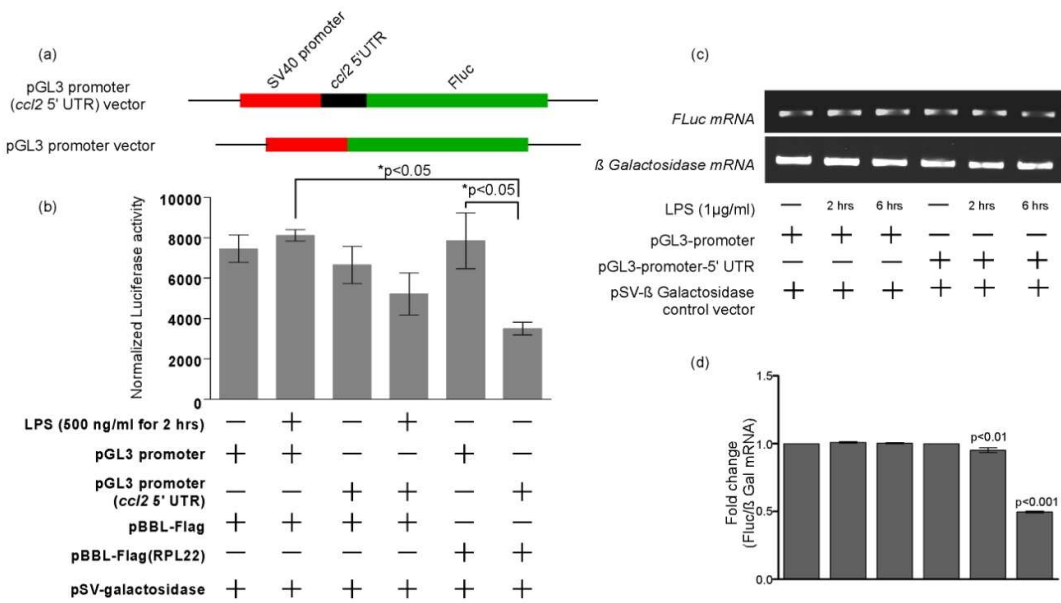


Figure 17: RPL22 down-grade luciferase activity and Fluc mRNA expression when ccl2 5' UTR was cloned upstream of luciferase ORF. 17a. linear map of 5' UTR cloned and uncloned pGL3-promoter vector. 17b. Luciferase assay was performed from vector transfected and LPS (1 μg/ml) treated or untreated MCF7 cells according to the manufacturer's protocol (Steady-Glo® Luciferase

Assay System, Promega, USA). The level of luciferase activity was normalized by ONPG-based beta-galactosidase activity from individual samples. 17c. The level of *Fluc* and beta-galactosidase mRNA was checked using semi-quantitative PCR in LPS (1 ug/ml) treated MCF7 cells. 17d. densitometric analysis of *Fluc* mRNA which was normalized by level of beta-galactosidase mRNA. Statistical analysis was performed by unpaired students' t-test using Gaph pad prism (online version. *** $p < 0.0005$, ** $p < 0.005$, * $p < 0.05$).

RPL22 binds to UPF-1 up on LPS-treatment- As RPL22 does not possess any nuclease activity by itself then how the binding of RPL22 on 5'UTR of *ccl2* mRNA leads to its degradation? To address this question we have pulled down RPL22 from LPS-treated and untreated THP-1 macrophages using anti-RPL22 antibody and performed LC-MS analysis (Figure 18a) with eluted samples. Result suggested that among other RNA-binding proteins, UPF-1 was co-eluted in LPS treated samples. To confirm this binding, we have performed *in vitro* binding assay with purified 6xHis tagged RPL22. A total of 100 µg purified His tagged RPL22 protein was allowed to bind with 100 µl of Hispure Ni-NTA superflow agarose beads (Pierce, USA) for 1 hr at 4° C in rotation (15 rpm). The beads were washed and mixed with 500 µg cell lysate prepared from LPS-stimulated and unstimulated THP-1 cells and and were incubated for 4 hr at 4° C. After washing, bound protein complexes were eluted and subjected to SDS-PAGE, followed by western blotting using anti-UPF-1 antibody. Result showed that UPF-1 can interact with bacterial expressed recombinant RPL22 *in vitro* in LPS-treated conditions (Figure 18b). We speculate that there may be any post translational modification of UPF-1 under LPS-treatment (17) is responsible for this binding. To understand RPL22-UPF-1 interaction in *in vivo* setup, we have co-transfected MCF7 cells with pcDNA3.1-RPL22-6XHis and pcDNA-UPF-1-Flag and post-transfection cells were either treated with LPS (1 µg/ml) for 2 hrs or left untreated. 6XHis-tagged RPL22 was pulled down by Ni-NTA agarose beads and following immunoblot using anti-UPF-1 revealed that UPF-1 interacted with RPL22 in LPS-untreated but over-expressed cells. However, LPS induction in co-transfected cells showed a significant increase in RPL22-UPF-1 interaction, which in turn consistent with our previous binding experiments (Figure 18c).

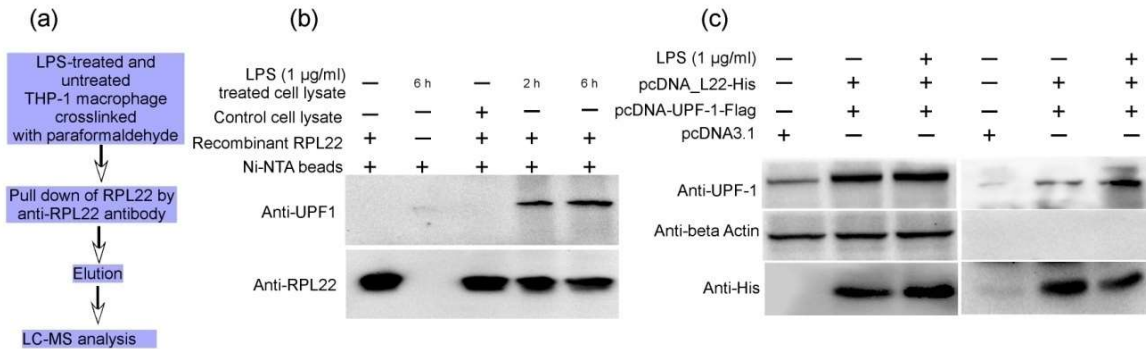


Figure 18: RPL22 binds to UPF-1 upon LPS treatment. 18a. THP-1 macrophages were either treated with LPS (100 ng/ml) for 2 hrs or kept untreated. Cell lysate from two samples were incubated with anti-RPL22 conjugated Sepharose protein G 4B beads (Invitrogen, USA). After washing, elutes were sent for LC-MS analysis. 18b. 6Xhis tagged purified recombinant RPL22 (100 ng) was fixed with Ni-NTA agarose beads (Pierce, USA) and LPS-treated and untreated THP-1 macrophage cell lysate

was passed through the beads. Immunoblot was performed with elutes using anti-RPL22 and anti-UPF-1 antibody. 18c. pcDNA-UPF1-Flag and pcDNA-L22-His were co-transfected into MCF7 cells and 48 hrs post transfection cells were treated with either LPS (1ug/ml) for 2 hrs or left untreated. 6XHis tagged RPL22 was pulled down with Ni-NTA agarose beads and elutes were immunoblotted with anti-His, anti-UPF-1 and anti-beta actin antibody.

We have checked the sub-cellular localization of RPL22 and UPF-1 under different time points of LPS treatment in MCF7 cells to understand the co-incident of these two proteins. Immunofluorescence study using anti-RPL22 and anti-UPF-1 antibody suggested that LPS (1 µg/ml) treatment induced RPL22 and UPF-1 to accumulate in the nucleus at 2 hrs of the treatment (Figure 19) in MCF7 cells (we have already checked nuclear accumulation of RPL22 under 2 hrs of LPS treatment in THP-1 macrophages). Untreated MCF7 cells has undetected amount of UPF-1 protein in nucleus while RPL22 was distributed throughout the cells. At 6 hrs hours of LPS-treatment, the nuclear accumulation of both the proteins was reduced as compared to the 2 hrs of LPS-treatment. The results suggested that these two proteins share same sub-cellular compartment under the LPS-challenge hinting the physical basis of interaction.

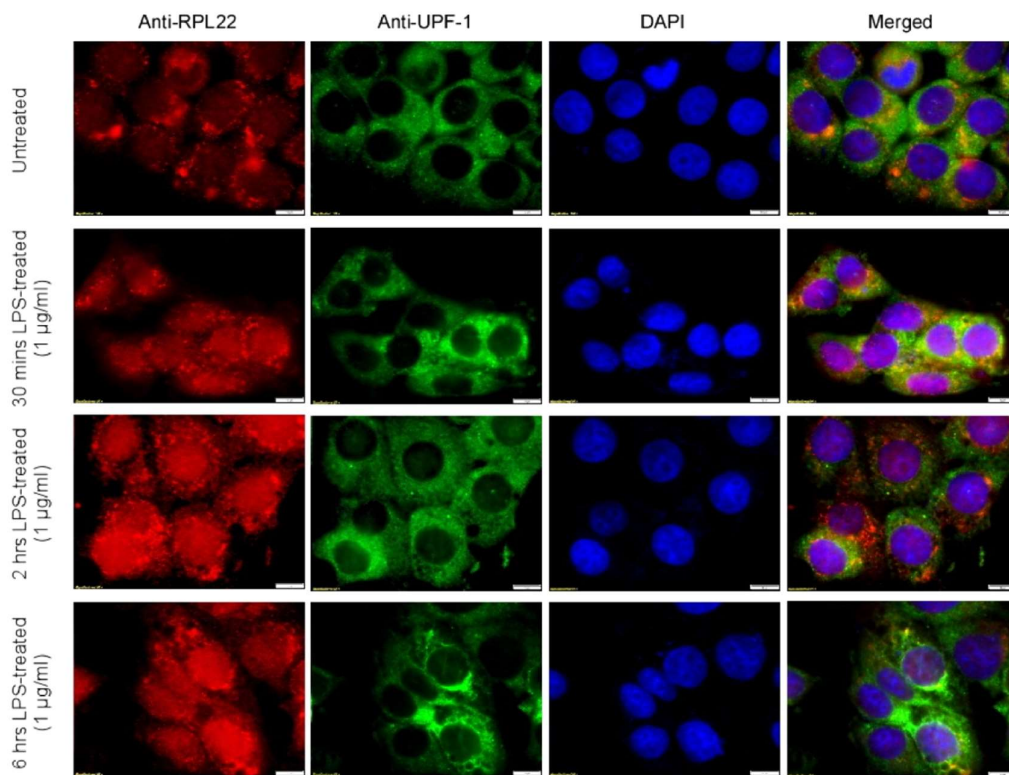


Figure 19: RPL22 and UPF-1 co-localizes inside nucleus in LPS-treated cells. MCF7 cells were grown in cover slips and treated with LPS (1 ug/ml) for 30 mins, 2 hrs and 6 hrs. Localization of RPL22 and UPF-1 proteins were checked by staining the cells with ant-RPL22 and ant-UPF-1 antibody. Cell images were acquired in 100X magnification (oil immersion) with same exposure. DAPI in mounting dye (AntiFade Gold, Invitrogen, USA) was used for staining the nucleus.

RPL22 and UPF-1 complex is responsible for ccl2 mRNA degradation in cytoplasm- We wanted to learn whether the RPL22-UPF-1 complex is responsible for ccl2 mRNA turnover. To understand this, we have transiently over-expressed (individually or together) RPL22 and UPF-1 in MCF7 cells and either treated with LPS (1 μ g/ml) or left untreated for 2 hrs of post-transfection. qRT-PCR analysis using ccl2 gene specific primer revealed that over-expression of RPL22 alone significantly down regulated ccl2 expression in both 2 hrs LPS untreated and treated cells as compared to empty pcDNA3.1(+) transfected LPS-untreated cells. This result was consistent with RPL22 KO cells where ccl2 mRNA accumulation was significantly increased upon LPS challenge as compared to the RPL22 wild type cells. However, only over-expression of UPF-1 could not able to significantly diminish ccl2 mRNA in LPS-untreated and treated cells. Interestingly, cells where both RPL22 and UPF-1 were over-expressed, showed significant lower level of ccl2 mRNA in LPS-untreated and treated conditions. Nevertheless, 2 hrs LPS-treatment on RPL22 and UPF-1 co-over-expressed cells showed a drastic lower level of ccl2 mRNA (fold change 0.14) as compared to the pcDNA3.1(+) transfected LPS-untreated cells (Figure 20). These results suggesting that LPS treatment induced ectopically expressed RPL22 and UPF-1 to translocate into nucleus individually or as a complex and led to the degradation of ccl2 mRNA by binding of RPL22 to the 5'UTR.

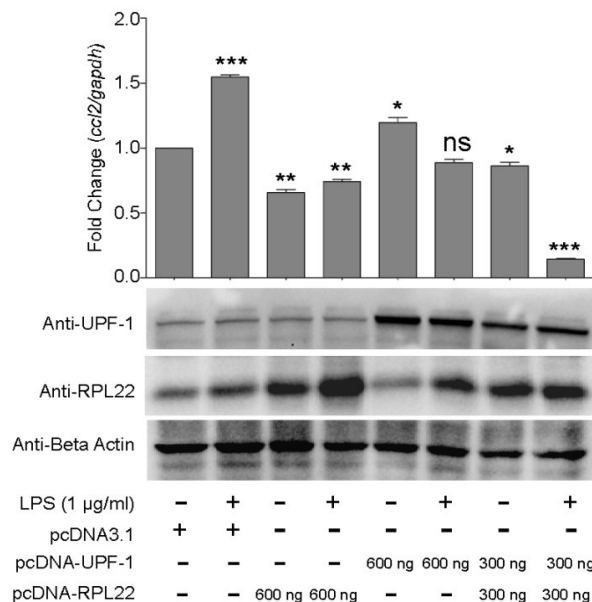


Figure 20: RPL22 and UPF-1 complex is responsible for ccl2 mRNA degradation. pcDNA-UPF-1-Flag and pcDNA-RPL22-His plasmids were co-transfected into MCF7 cells. Forty eight hours post-transfection cells were treated with LPS (1 μ g/ml) for 2 hrs. The level of RPL22 and UPF-1 was checked by western blotting against anti-RPL22 and anti-UPF-1 antibody respectively. The amount of ccl2 mRNA in each sample was checked using ccl2 gene specific primers using real time PCR (ABI7500, Applied Biosystems, USA). Statistical

analysis was performed by comparing treated samples with control sample by unpaired students' t-test using Gaph pad prism (online version. *** $p < 0.0005$, ** $p < 0.005$, * $p < 0.05$).

Now we tried to validate the fact that absence of either UPF-1 or RPL22 or both have any opposite effect on *ccl2* mRNA abundance. To study this, we have transfected THP-1 macrophages with either scrambled siRNA, UPF-1 siRNA (Sigma, USA) or both RPL22 and UPF-1 siRNA using Lipofectamine RNAiMAX (Invitrogen, USA). Forty eight hours post-transfection, cells were treated with either left untreated or treated with LPS (100 ng/ml) for 2 hrs. Cells were harvested in TRIZOL and total RNA was extracted followed by DNaseI treatment (Thermo Fisher, USA) for 30 mins at 37 °C. The DNaseI treated samples were then re-extracted with TRIZOL and cDNA was synthesized using Verso cDNA synthesis Kit (Thermo, USA). The level of *ccl2* mRNA was checked by real time PCR using *ccl2* gene specific primers. *gapdh* mRNA was taken as endogenous control for each samples. Result showed that LPS induction could induce *ccl2* mRNA expression in scrambled siRNA transfected THP-1 macrophages to a 131.81 fold as compared to the untreated cells (Figure 21c). Interestingly only UPF-1 siRNA transfected THP-1 cells significantly (* $p < 0.05$) induced *ccl2* mRNA (fold change 23.56) as compared to the scrambled siRNA transfected but untreated cells. *ccl2* mRNA was further increased significantly (* $p < 0.05$) when UPF-1 siRNA transfected THP-1 cells were challenged with 100 ng/ml LPS for 2 hrs (Fold change 137.48). These result suggested that knock down of UPF-1 (we have checked the knock down efficiency to be 50% to the wild type cells, Figure 21a, b) induced *ccl2* mRNA hinting that low level of UPF-1 prevented the turnover of *ccl2* mRNA. However, role of UPF-1 has been attributed in the regulation of normal *ccl2* mRNA turnover (18). So we have speculated that down regulation of UPF-1 may have RPL22-independent effect on *ccl2* mRNA stability. To defy this possibility, we have co-transfected THP-1 macrophages with RPL22 siRNA and UPF-1 siRNA and post-transfection cells were either treated with LPS (100 ng/ml) for 2 hrs or left untreated. The *ccl2* mRNA amount was significantly (** $p < 0.005$) up-regulated untreated cells co-transfected with the siRNAs as compared to the scrambled siRNA transfected untreated cells (fold change 48.45). Further LPS treatment on the co-transfected cells induced a robust (* $p < 0.05$) expression of *ccl2* mRNA as compared to the controls (fold change 279.23) (Figure 21c). These results suggested that RPL22-UPF-1 complex is responsible for the degradation of *ccl2* mRNA.

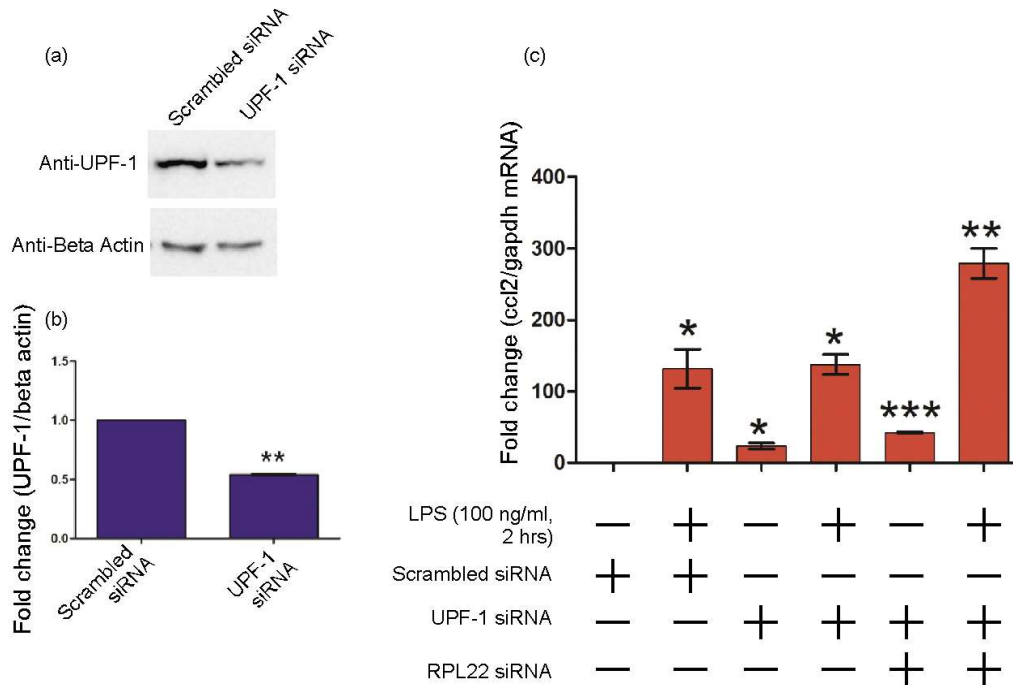


Figure 21: Knock down of RPL22-UPF-1 complex increases *ccl2* mRNA. 21a, b. THP-1 macrophages were transfected with UPF-1 siRNA (Sigma, USA) using Lipofectamine RNAiMAX (Invitrogen, USA) for 48 hrs. The knock down efficiency of UPF-1 protein was checked by immunoblotting the cell lysate against anti-UPF-1 antibody. 21b. THP-1 macrophages were treated with RPL22 siRNA and UPF-1 siRNA according to previously described method. Transfected cells were treated with LPS (100 ng/ml) for 2 hrs and *ccl2* mRNA abundance was checked using *ccl2* gene specific primers by real time PCR. Statistical analysis was performed by comparing treated samples with control sample by unpaired students' t-test using Gaph pad prism (online version. *** $p < 0.0005$, ** $p < 0.005$, * $p < 0.05$).

Next, we asked the site of degradation of the mRNA degradation. To elucidate this, we have first checked involvement of CRM-1 for nuclear export of RPL22 and UPF-1 in our condition. Though previous reports suggested that UPF-1 shuttles through CRM-1 (19-21), there was no concrete evidence on nuclear exporter of RPL22. We have treated MCF7 cells with Leptomycin B (LMB, 20 μ M) 20 mins after the LPS treatment (1 μ g/ml, 2 hrs) and have separated nucleus and cytoplasm. Our result revealed that LPS-induction followed by LMB treatment significantly mustered both RPL22 and UPF-1 nucleus as compared to the only LPS treatment, suggesting CRM-1 is responsible for nuclear export of both the proteins (Figure 22a). Furthermore, we checked *ccl2* turnover kinetics with or without blocking the CRM-1 by LMB. We have treated THP-1 macrophages with LMB (20 μ M) 20 mins prior to LPS (1 μ g/ml, for 2 hrs) treatment followed by ActD (5 μ M) treatment up to 6 hrs. Our result suggested that in presence of LMB, the *ccl2* mRNA was stable even at the 6 hrs of ActD treatment (Figure 22b). When the CRM-1 was not blocked (absence of LMB), *ccl2* mRNA was degraded as we have seen in the previous experiments (Figure 22c). These results suggested that *ccl2* mRNA complexed with RPL22 and UPF-1 leaves the nucleus after 2 hrs of LPS treatment and degrade the mRNA in the cytoplasm.

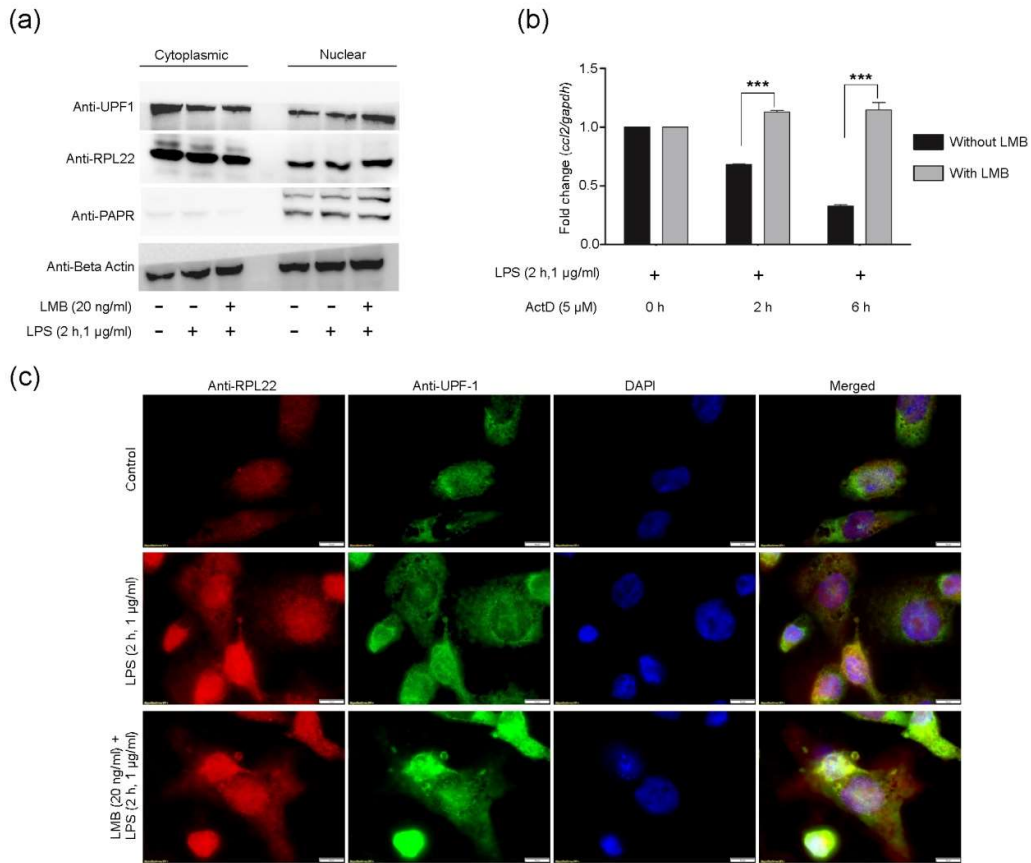


Figure 22: RPL22-UPF-1 complex degrades *ccl2* mRNA in cytoplasm in LPS mediated inflammation. 22a. MCF7 cells were treated with LMB (20 ng/ml) and LPS (1 µg/ml) for 2 hrs and nuclear and cytoplasm was separated according to the manufacturer's protocol (NE-PER™ Nuclear and Cytoplasmic Extraction Reagents, Pierce, USA). RPL22 and UPF-1 was immunoblotted using anti-RPL22 and anti-UPF-1 antibody. 22b. MCF7 cells were treated with LMB and LPS as the previous experiment and then global transcription was blocked by treating the cells with Actinomycin D (5 µg/ml) for 2 hrs and 6 hrs. *ccl2* mRNA was checked in each sample using *ccl2* gene specific primers in real time PCR. 22c. THP-1 macrophages were grown in cover slips and treated with only LPS (1 µg/ml) or LMB (20 ng/ml) and LPS (1 µg/ml) for 2 hrs and cellular locations of RPL22 and UPF-1 was checked by staining the cells with anti-RPL22 and anti-UPF-1 antibody and visualizing the in 100X magnification (oil immersion) using blue and green filter respectively. DAPI in mounting dye was used for staining the nucleus. Statistical analysis was performed by unpaired students' t-test using Gaph pad prism (online version). *** $p < 0.0005$, ** $p < 0.005$, * $p < 0.05$.

RPL22 requires 20 nucleotides for binding to the 5'UTR of *ccl2* mRNA-To understand the minimal binding requirement for RPL22 on the *ccl2* mRNA, we have performed RNA-protein cross-linking experiments using deletion constructs. From the 65 bp 5'UTR of *ccl2* mRNA we have generated three synthetic oligos (a, b and c) having T7 promoter and produced the RNA fragments using *in vitro* transcription (Figure 23a). Result from the cross-linking experiment showed that RPL22 could able to bind to deletion constructs **a and d** as well as to the whole 65 bp 5'UTR while construct **c** was not able to bind to the protein. From

this experiment we have concluded that first 20 bp of the 5'UTR possess the RPL22 binding site (Figure 23b). To understand the global distribution of RPL22 binding site in the human transcriptome, we have performed BLAST analysis by using 5'GAGAGGCUGAGACUAACCCA3' sequence as query. Result showed that the RPL22 binding sequence matches >70% with 7 other cellular mRNA sequences in the Human transcriptome (Figure 23c). Remarkably *ccl11* (Eotaxin-1) shares 95% sequence similarity with 20 nt RPL22 binding site on *ccl2* mRNA, which is an eosinophil chemo-attractant protein. To confirm the interaction between RPL22 and 7 other transcripts we have performed RNA-ChIP experiment. Result showed that RPL22 can bind to *ccl11*, *prlr* mRNAs suggesting a common mode of regulation by RPL22 (Figure 23d). To understand biological significance of RPL22 binding to *ccl11*, *sh2b1*, *unc5b* and *prlr* mRNAs, we have checked their mRNA level in absence of RPL22. qRT-PCR analysis showed that the level of uninduced and LPS-induced mRNA was significantly increased in case of *ccl11* and *prlr* in RPL22 KO MCF7 cells as compared to the WT MCF7 cells with respective treatment

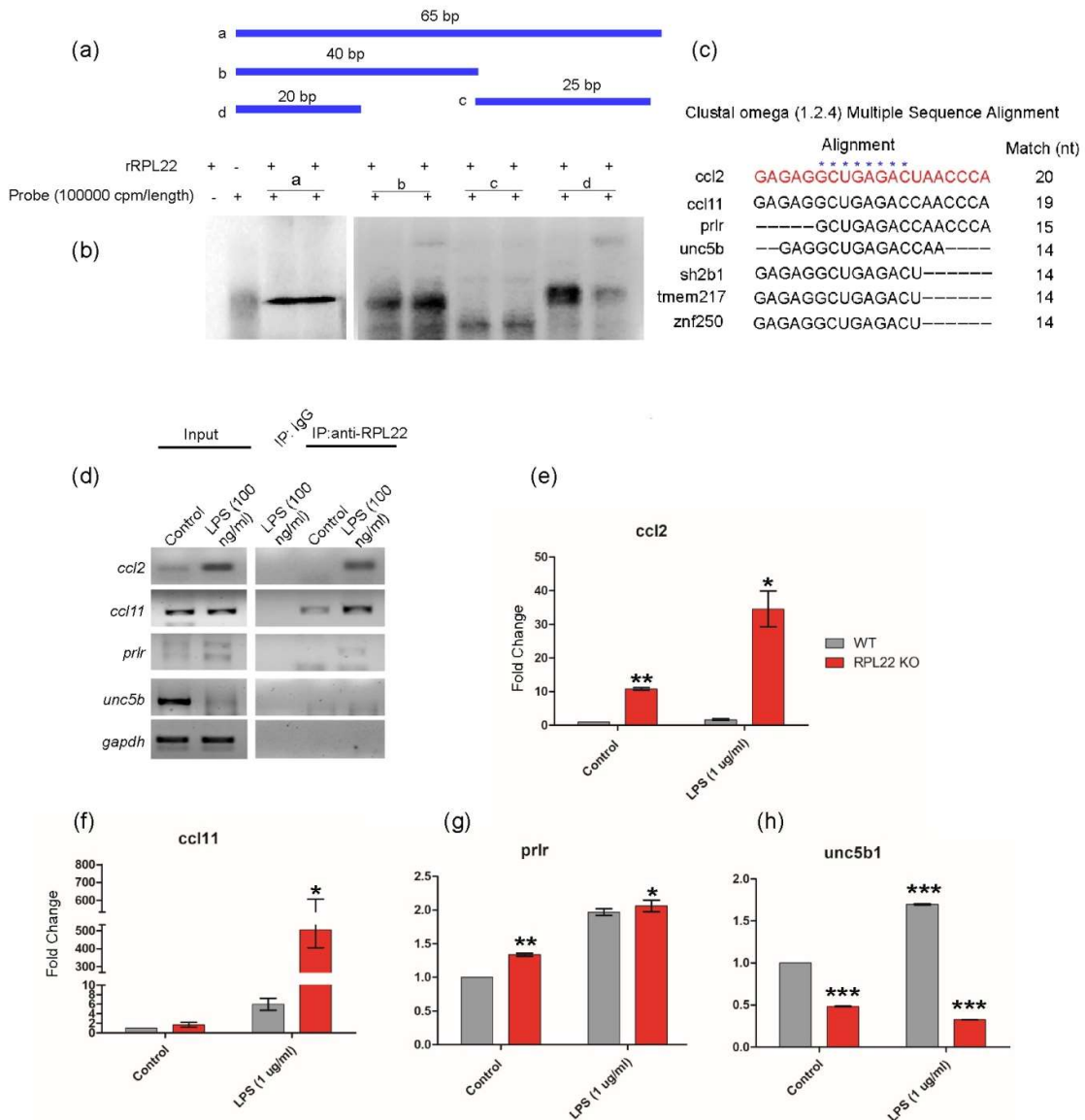


Figure 23: **RPL22 requires 20 nucleotides for binding to the 5'UTR of ccl2 mRNA.** 23a. Deletion construct (mRNAs) were made by *in vitro* transcription from 5' UTR of *ccl2* mRNA and body labeled by radiolabelled rUTP. 23b. UV-crosslinking assay was performed with human recombinant RPL22 protein. 23c. the minimal binding sequence of RPL22 (20 nt) was matched with Human Transcriptome database (NCBI) using Nucleotide Blast online server of NCBI. 23d. Selected genes were checked for its binding to RPL22 *in vivo* by RNA-CLIP assay in LPS-treated THP-1 macrophages. 23e,f,g, h. *ccl2*, *ccl11* *prlr* and *unc5b* gene expression was checked in RPL22 WT and RPL22 KO MCF7 cells. Statistical analysis was performed by unpaired students' *t*-test using Gaph pad prism (online version. ****p*<0.0005, ***p*<0.005, **p*<0.05.

conditions. While the expression of *unc5b* was significant diminished in RPL22 KO cells (LPS-treated and untreated) with respect to the WT cells (Figure 23 e,f,g,h). This result further suggested RPL22 may act as an important regulon by restricting cells to be overwhelmed by inflammatory signaling.

RPL22 regulates monocyte migration -To understand the biological significance of RPL22 binding to *ccl2* mRNA and its subsequent degradation, we have performed chemotaxis assay Briefly, the lower compartments (Costar #3421; Corning Incorporated, Corning, NY) of each well were seeded with either WT, RPL22 (KO) MCF7 cells or PMA differentiated WT and RPL22 OE THP-1 macrophages in 1% BSA supplemented RPMI 1640 media. The THP-1 monocyte cells were adjusted to the cell density of 1×10^6 cells/ml, 100,000 cells in 200 μ l 1

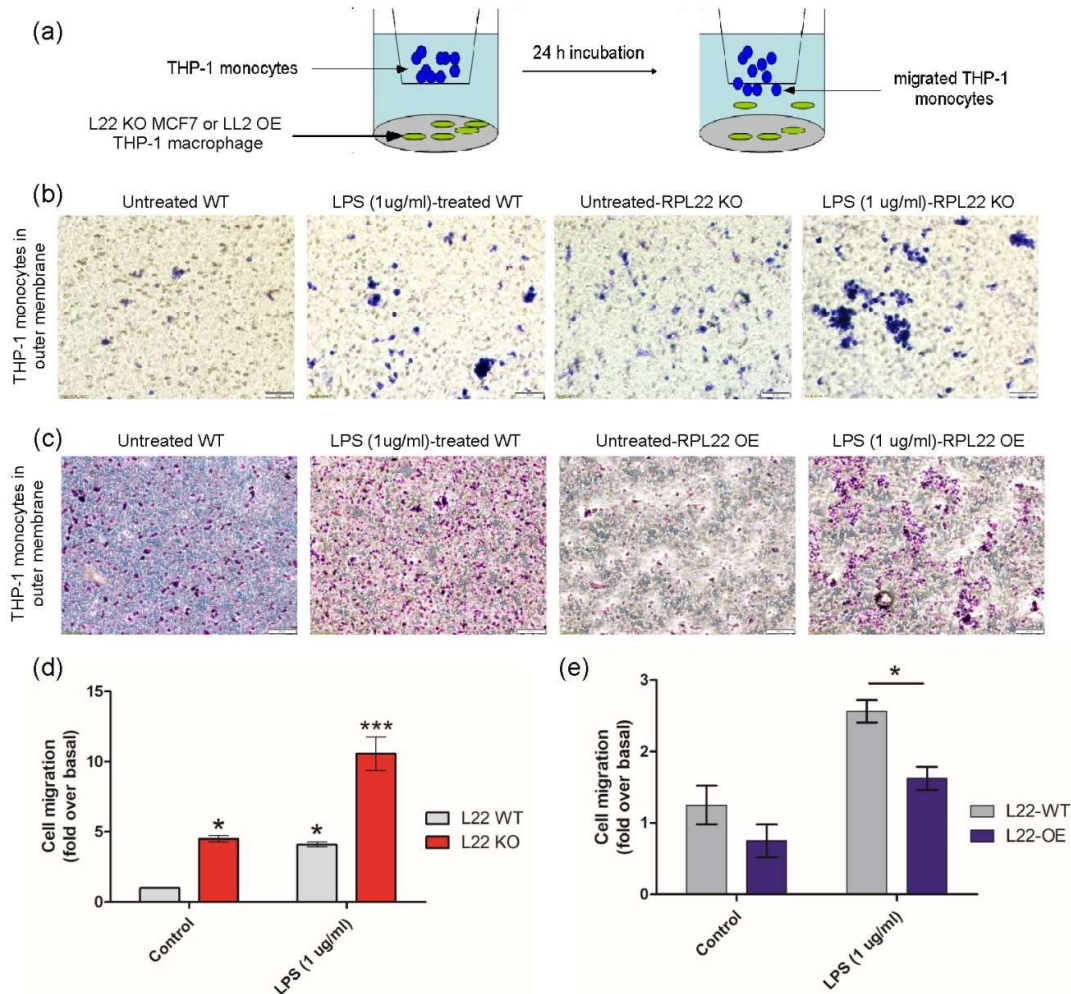


Figure 24: RPL22 regulates monocyte migration in LPS-mediated inflammation. 24a. Schematic representation of migration assay using Transwell inserts (pore size: 5 μ M, Corning, USA). 24b. THP-1 monocyte migration was checked by co-culturing MCF7 WT and MCF7 RPL22 KO cells either untreated or treated with LPS (1 μ g/ml) for 2 hrs. 24c. THP-1 monocyte migration was checked by co-culturing WT THP-1 macrophages and RPL22 overexpressed THP-1 macrophages either untreated or treated with LPS (1 μ g/ml) for 2 hrs. 24d, e. Percent of cells migrated to the outer surface of transwell membrane was counted (at least 10 fields) of both the experiments and plotted against cells migrated in control samples. Statistical analysis was performed by unpaired students' t-test using Graph pad prism (online version. *** $p < 0.0005$, ** $p < 0.005$, * $p < 0.05$).

% BSA containing RPMI media were added to the top chamber of a 24-transwell apparatus (6.5 mm in diameter, 5.0 μ m pore size) and allowed for migration for 24 h at 37 °C in 5% CO₂ (Figure 24a). Then the cells were fixed with 3.7% paraformaldehyde for 2-3 minutes at RT followed by washing with PBS. Later, the cells were permeabilized using 100% methanol for 20 minutes at room temperature and washed again with PBS. Finally, cells were stained with 0.05% crystal violet in PBS for 15 minutes at RT. Cells on the upper side of the filters were removed with cotton swabs, while the lower sides were counted under a microscope in six randomly selected visual fields in each well. The result suggested LPS-untreated and treated RPL22 KO MCF7 cells attracted a significant amount of monocytes as compared to the WT MCF7 cells in respective conditions (Figure 24b, d). We have observed opposite effect of RPL22 OE cells on the migration of monocytes from the upper chamber. Over-expression of RPL22 significantly repressed monocyte migration in both LPS –treated and untreated cells as compared to the control or LPS-treated empty vector transfected cells (Figure 24c, e).

B2. Summary and Conclusions of the Progress made so far (minimum 100 words, maximum 200 words):

Several recent literatures confirmed ‘moonlighting’ function of ribosomal proteins (RPs) in addition to its canonical role in ribosome biogenesis and translation. The current project aimed at studying role of RPs in inflammation, a form of adaptive response against noxious stimuli such as pathogens, chemicals or physical injury. Transcriptomics profiling of

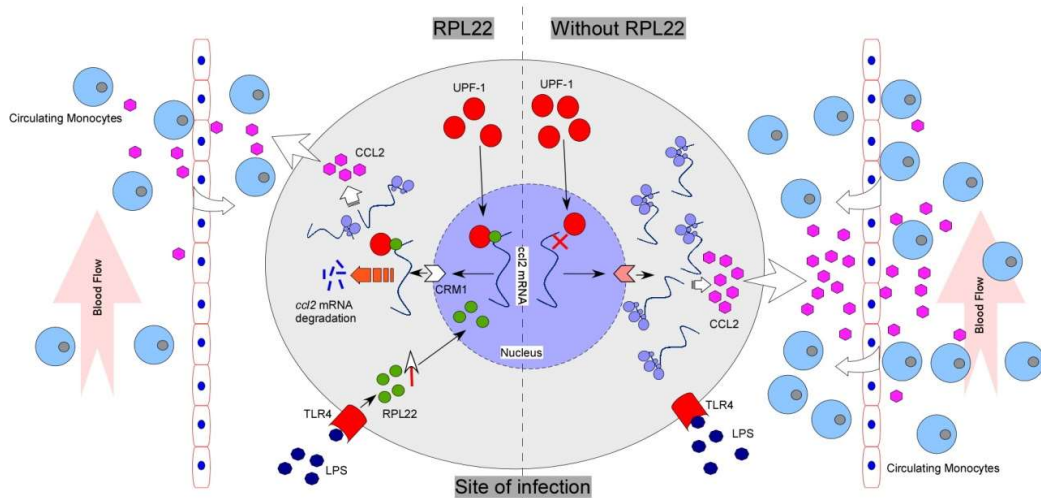


Figure 25: Schematic representation of the RPL22-mediated regulation of ccl2 mRNA

ribosomal proteins (RPs) revealed significant up-regulation of large ribosomal subunit protein L22 in differentiated human monocytic THP-1 cells following stimulation with bacterial LPS. Interestingly, L22 expression remained unaltered when cells were treated with IL-6 or TNF α , suggesting its association with bacterial infection. To investigate the role of L22 in inflammation, ribo-immunoprecipitation (RIP) assay was performed using anti-L22 antibody followed by RT-PCR with a series of inflammatory gene-specific primers. L22 was found to specifically interact with the mRNA of CCL2 (also known as MCP-1), a well characterized inflammatory mediator. Overexpressed L22 translocated into nucleus where it binds to *ccl2* mRNA. We have mapped the site of L22 binding site on the *ccl2* mRNA. Our results suggest that only 20 nucleotides on the 5'UTR of *ccl2* mRNA is the minimal requirement for L22 binding. The L22-*ccl2* mRNA complex facilitates UPF-1 to bind to *ccl2* mRNA via interaction with L22. This RNP complex exit the nucleus via CRM1 exporter leading to degradation of the *ccl2* mRNA. Stabilization of the LPS-stimulated *ccl2* transcript in CRISPR-Cas9 mediated L22-deficient cells confirmed the role of L22 in this mechanism. Thus, unusual high expression of CCL2 protein was observed in L22-deficient cells suggesting critical role of L22 as a post-transcriptional check point for CCL2 expression. There are possibilities that this function of RPL22 as a 'watchdog' for regulation of several other inflammatory transcripts is a component of a 'regulome' to check inflammatory responses under control. Our study thus suggests a novel function of L22-mediated degradation of CCL2 mRNA and contributes to the mounting evidences of regulatory functions of RPs.

B3. Details of New Leads Obtained, if any:

- A non-canonical role of a ribosomal protein (RPL22) has been identified.
- RPL22 post-transcriptionally regulate C-C motif chemokine ligand 2 (*ccl2*) expression thereby renders controlled monocyte-infiltration to the site of bacterial infection
- *ccl11*, an eosinophil chemo-attractant protein, having 95% similar L22 binding sequence (20 nt) as *ccl2*, is also regulated by L22 suggesting global role of this RP in macrophage migration

B4. Details of Publications, technology developed & Patents, if any emanated from the project:

- i. Post-transcriptional regulation of C-C motif chemokine ligand 2 expression by ribosomal protein L22 during LPS-mediated inflammation- Das AS, Basu A, Kumar R, Borah PK, Bakshi S, Sharma M, Duary RK, Ray PS and Mukhopadhyay R (Under revision).
- ii. Comparative transcriptomics of infectious and non-infectious systemic inflammation: Correlation with antibody therapy against rheumatoid arthritis- Das AS, Sarkar A, Basu A, Sharma M, Ghosh Z and Mukhopadhyay R (Communicated).
- iii. *Ricinus communis* L. fruit extract inhibits migration/invasion, induces apoptosis in breast cancer cells and arrests tumor progression *in vivo*- Majumder M, Debnath S, Gajbhiye RL, Saikia R, Gogoi B, Samanta SK, Das DK, Biswas K, Jaisankar P &

- Mukhopadhyay R, *Scientific Reports*, 9:14493, 2019 (<https://doi.org/10.1038/s41598-019-50769-x>)
- iv. STAT3 and NF- κ B are Common Targets for Kaempferol-mediated Attenuation of COX-2 Expression in IL-6-induced Macrophages and Carrageenan-induced Mouse Paw Edema- Basu A, Das AS, Sharma M, Pathak MP, Chattopadhyay P, Biswas K and Mukhopadhyay R, *Biochem. Biophys Rep*, 12, 54-61, 2017.
- v. Anti-atherogenic Role of Chrysin, Quercetin and Luteolin- Basu A, Das AS, Majumder M and Mukhopadhyay R, *J. Cardiovasc. Pharmacol.*, **68**, 89-96, 2016.

B5. Benefits gained through U-Excel:

- *Scientific & Technical expertise gained through U Excel in NER:* The U Excel project has provided an excellent opportunity for the scientists in NER to venture deep into new and exciting problems which otherwise would not have been possible. Scientifically this project helped us to set up several facilities e.g. cell culture facility, fluorescence imaging facility, ultracentrifugation facility and qPCR facility. These facilities led to training of manpower in the field of cell and molecular biology.
- *No. of NER manpower (including PI & staffs) trained in the Non-NER Institute:* One
- *No. of visits by Non-NER Researchers to NER Institutes and vice-versa:* N/A
- *Training in any new techniques, if any:* The students were trained with several new and state-of-the-art techniques for carrying out the objectives of the project. These include and not limited to polysome fractionation, Knock out of proteins in cells using CRISPR-Cas9 system, Co-localization studies, mRNA-protein binding studies, basic bioinformatics studies, gene expression analysis using qPCR and western blots. **In addition, a 2-days workshop cum training program has been organized from U Excel funds to give hands on training to research scholars/young faculties during November 25-26, 2017. A separate report on the program has been attached at the end of this document (Annexure I).**

Section-C: Details of Grant Utilization^{#±}

C1. Equipment Acquired or Placed Order with Actual Cost: Attached a list of instrument procures under the grant duly certified from the competent authority.

C2. Manpower Staffing and Expenditure Details: Kindly refer to UC/SE

C3. Details of Recurring Expenditure: Kindly refer to UC/SE

C4. Financial Requirements for the Next Year with Justifications: N/A

#Grant utilization details (UC&SE, Assets Certificate & manpower details) also required to be submitted separately as per the prescribed format

± (The information for Section-C will be submitted as the final UC-SE of the project)

(Dr. Rupak Mukhopadhyay)

[Signature(s) of the Investigator]

References:

1. Kruth HS, Huang W, Ishii I, Zhang W-Y. Macrophage foam cell formation with native low density lipoprotein. *Journal of Biological Chemistry*. 2002;277(37):34573-80.
2. Rahaman SO, Lennon DJ, Febbraio M, Podrez EA, Hazen SL, Silverstein RL. A CD36-dependent signaling cascade is necessary for macrophage foam cell formation. *Cell metabolism*. 2006;4(3):211-21.
3. Ricote M, Huang JT, Welch JS, Glass CK. The peroxisome proliferator-activated receptor γ (PPAR γ) as a regulator of monocyte/macrophage function. *Journal of leukocyte biology*. 1999;66(5):733-9.
4. Moore KJ, Sheedy FJ, Fisher EA. Macrophages in atherosclerosis: a dynamic balance. *Nature Reviews Immunology*. 2013;13(10):709.
5. Quandt K, Frech K, Karas H, Wingender E, Werner T. MatInd and MatInspector: new fast and versatile tools for detection of consensus matches in nucleotide sequence data. *Nucleic acids research*. 1995;23(23):4878-84.
6. Malygin AA, Parakhnevitch NM, Ivanov AV, Eperon IC, Karpova GG. Human ribosomal protein S13 regulates expression of its own gene at the splicing step by a feedback mechanism. *Nucleic acids research*. 2007;35(19):6414-23.
7. Macías S, Bragulat M, Tardiff DF, Vilardell J. L30 binds the nascent RPL30 transcript to repress U2 snRNP recruitment. *Molecular cell*. 2008;30(6):732-42.
8. Vilardell J, Warner JR. Regulation of splicing at an intermediate step in the formation of the spliceosome. *Genes & development*. 1994;8(2):211-20.
9. Dobbstein M, Shenk T. In vitro selection of RNA ligands for the ribosomal L22 protein associated with Epstein-Barr virus-expressed RNA by using randomized and cDNA-derived RNA libraries. *Journal of virology*. 1995;69(12):8027-34.
10. Toczyński DP, Matera AG, Ward DC, Steitz JA. The Epstein-Barr virus (EBV) small RNA EBER1 binds and relocalizes ribosomal protein L22 in EBV-infected human B lymphocytes. *Proceedings of the National Academy of Sciences*. 1994;91(8):3463-7.
11. Rashkovan M, Vadnais C, Ross J, Gigoux M, Suh W-K, Gu W, et al. Miz-1 regulates translation of Trp53 via ribosomal protein L22 in cells undergoing V (D) J recombination. *Proceedings of the National Academy of Sciences*. 2014;111(50):E5411-E9.
12. Jung HI, Bowden SJ, Cooper A, Perham RN. Thermodynamic analysis of the binding of component enzymes in the assembly of the pyruvate dehydrogenase multienzyme complex of *Bacillus stearothermophilus*. *Protein science : a publication of the Protein Society*. 2002;11(5):1091-100.
13. Salim NN, Feig AL. Isothermal titration calorimetry of RNA. *Methods*. 2009;47(3):198-205.
14. Schmittgen TD, Zakrajsek BA, Mills AG, Gorn V, Singer MJ, Reed MW. Quantitative reverse transcription-polymerase chain reaction to study mRNA decay: comparison of endpoint and real-time methods. *Analytical biochemistry*. 2000;285(2):194-204.
15. Wang Y, Rangan GK, Goodwin B, Tay Y-C, Wang Y, Harris DC. Lipopolysaccharide-induced MCP-1 gene expression in rat tubular epithelial cells is nuclear factor- κ B dependent. *Kidney international*. 2000;57(5):2011-22.

16. Anand AR, Bradley R, Ganju RK. LPS-induced MCP-1 expression in human microvascular endothelial cells is mediated by the tyrosine kinase, Pyk2 via the p38 MAPK/NF- κ B-dependent pathway. *Molecular immunology*. 2009;46(5):962-8.
17. Durand S, Franks TM, Lykke-Andersen J. Hyperphosphorylation amplifies UPF1 activity to resolve stalls in nonsense-mediated mRNA decay. *Nature communications*. 2016;7:12434.
18. Cho H, Park OH, Park J, Ryu I, Kim J, Ko J, et al. Glucocorticoid receptor interacts with PNRC2 in a ligand-dependent manner to recruit UPF1 for rapid mRNA degradation. *Proceedings of the National Academy of Sciences*. 2015;112(13):E1540-E9.
19. Higa M, Oka M, Fujihara Y, Masuda K, Yoneda Y, Kishimoto T. Regulation of inflammatory responses by dynamic subcellular localization of RNA-binding protein Arid5a. *Proceedings of the National Academy of Sciences*. 2018:201719921.
20. Mendell JT, Ap Rhys CM, Dietz HC. Separable roles for rent1/hUpf1 in altered splicing and decay of nonsense transcripts. *Science*. 2002;298(5592):419-22.
21. Ajamian L, Abel K, Rao S, Vyboh K, García-de-Gracia F, Soto-Rifo R, et al. HIV-1 recruits UPF1 but excludes UPF2 to promote nucleocytoplasmic export of the genomic RNA. *Biomolecules*. 2015;5(4):2808-39.

Annexure I

Documents on Training cum Workshop

Organized from

DBT U-Excel project: “Role of non-canonical function
of ribosomal proteins in inflammation”
(BT/410/NE/U-Excel/2013)

Utilisation Certificate

(for the financial year ending 31st March 2018)
(01/04/2017 to 31/03/2018)

(Rs. in Lakhs)

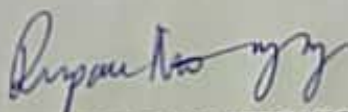
1. Title of the Project/Scheme: **Role of non-canonical function of ribosomal proteins in inflammation**
2. Name of the Organization: **Tezpur University**
3. Principal Investigator: **Dr. Rupak Mukhopadhyay**
4. Deptt. of Biotechnology sanction order No. & date of sanctioning the project: **BT/410/NE/U-Excel/2013 dated 06/02/2014**
5. Amount brought forward from the Previous financial year quoting DBT letter No. & date in which the authority to carry forward the said amount was given: **Rs. 14.46942 lakhs, BT/410/NE/U-Excel/2013 dated December 2nd, 2016.**
6. Amount received from DBT during the financial year (please give No. and dates of sanction orders showing the amounts paid): **NA**
7. Other receipts/interest earned, if any, on the DBT grants: **Rs. 0.00581 Lakhs**
8. Total amount that was available for Expenditure during the financial year (Sl. Nos. 5,6 and 7): **Rs. 14.47523 lakhs**
9. Actual expenditure (excluding commitments) incurred during the financial year (statement of expenditure is enclosed): **Rs. 14.24725 lakhs**
10. Unspent balance refunded, if any (Please give details of cheque No. etc.): **NIL**
11. Balance amount available at the end of the financial year: **Rs. 0.22798 lakhs**
12. Amount allowed to be carried forward to the next financial year vide letter No. & date: **Rs.0.22798 lakhs**

Rupak Mukhopadhyay
4/3/2020

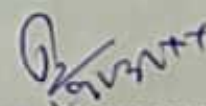
1. Certified that the amount of **Rs. 14.24725 lakhs** mentioned against col. 9 has been utilised on the project/scheme for the purpose for which it was sanctioned and that the balance of **Rs. 0.22798 lakhs** remaining unutilized at the end of the year has been surrendered to Govt. (vide No. Dy No. dated.....)/will be adjusted towards the grants-in-aid payable during the next year.
2. Certified that I have satisfied myself that the conditions on which the grants-in-aid was sanctioned have been duly fulfilled/are being fulfilled and that I have exercised the following checks to see that the money was actually utilised for the purpose for which it was sanctioned.

Kinds of checks exercised:

1. (Cash Book)
2. (Ledgers)
3. (Vouchers)
4. (Bank Statements)
- 5.

 4/13/2020
(PROJECT INVESTIGATOR)
Dr. RUPAK MUKHOPADHYAY
Assistant Professor
Department of M B B T
TEZPUR UNIVERSITY
Napaam, Tezpur, Assam, 784028


(FINANCE OFFICER)
Finance Officer
Tezpur University


(HEAD OF THE INSTITUTE)
Registrar
Tezpur University
Napaam, Tezpur

(To be countersigned by the DBT Officer-in-charge)

**FINAL CONSOLIDATED STATEMENT OF EXPENDITURE
(FOR FINAL SETTLEMENT OF ACCOUNTS)**

1. Title of the Project : Role of non-canonical functions of Ribosomal proteins in Inflammation
2. Sanctioned Project Cost : 152.07 Lakhs
3. Revised cost, if any : 147.58951
4. Duration of the project : 06/02/2014 to 31/03/2018
5. Sanction Order No. & Date : BT/410/NE/U-Excel/2013, Dated: 06/02/2014
6. Date of commencement of Project : 06/02/2014
7. Extension, if any : 06/02/2017 to 31/12/2017 and 01/01/2018 to 31/03/2018
8. Date of completion of project : 31/03/2018

Details of grant, expenditure and balance

S. No	Heads	Sanctioned Cost	Year-wise Releases made				Total	Year-wise Expenditure incurred						Total	Balance
			1 st yr	2 nd yr	3 rd yr	4 th Yr		6/2/14 31/3/14	1/4/14 31/3/15	1/4/15 31/3/16	1/4/16 31/3/17	1/4/17 31/3/18			
A. Non-recurring															
	Equipments	99.87	99.87	-2.17	0.00	0.00	97.70000	0.00	76.45975	21.23693	0.00	0.00	0.00	97.69668	0.00332
B. Recurring															
1.	Manpower	13.20	4.22	1.87 + 4.51	5.69	0.0	16.29000	0.00	3.21428	5.41193	4.88900	2.77479	16.29000	0.00	
2.	Consumables	32.00	11.00	10.11 - 2.34	9.03	0.0	27.80000	0.00	10.10836	7.69147	0.12973	9.99996	27.92952	-0.12952	
3.	Travel	1.00	0.40	-0.10000	0.07	0.0	0.37000	0.00	0.00	0.07321	0.17749	0.07896	0.32966	0.04034	
4.	Contingency	3.00	1.0	0.06 + 0.41790	1.0	0.0	2.47790	0.06604	0.78792	0.84905	0.39678	0.36219	2.46198	0.01592	
5.	Overhead	2.00	1.0	0.25 + 0.10	0.18 + 0.13	0.0	1.66000	0.00	0.94484	0.21875	0.45875	0.03305	1.65539	0.00461	
6.	Training	1.0	0.0	0.0	1.0	0.0	1.00000	0.00	0.00	0.00	0.00	0.99830	0.99830	0.00170	
7.	Interest	0.0	0.0	0.0	0.41580 - 0.13	0.00581	0.29161	0.00	0.00	0.00	0.00	0.00	0.00	0.29161	
	Total	52.2	17.62	14.8779	17.38580	0.00581	49.88951	0.06604	15.0554	14.24441	6.05175	14.24725	49.66485	0.22798	

[Handwritten Signature]
13/12/2018

Grand Total (A+B)	152.07	117.49	12.70790	17.38580	0.00581	147.58951	0.06604	91.51515	35.48134	6.05175	14.24725	147.36153	0.22798
----------------------	--------	--------	----------	----------	---------	-----------	---------	----------	----------	---------	----------	-----------	---------

Re-Appropriation of funds as per DBT's directions:

(2015-2016):

*Out of Rs.23.41 lakhs balance under NR head Rs. 18.90 lakhs is committed exp. And the remaining amount of Rs. 4.51 lakhs has been re-appropriated to Manpower head.

** Balance of Rs. 0.10 lakhs under the Travel head is re-appropriated to overhead charges.

***Interest earned of Rs. 1.04 (assuming 4% Balance Rs. 25.91) has been re-appropriated to overhead charges (Rs. 0.25) and contingency head (Rs. 0.75 lakhs)

(2016-2017):

*Interest earned of Rs. 0.13 lakhs (assuming 4% balance Rs. 3.13 lakhs) is re-appropriated to overhead.

Additional Bank Interest generated:

*Amount of Rs. 0.41580 was earned during FY (2016-2017)

**Amount of Rs. 0.00581 was earned during FY (2017-2018)

Rupak Mukhopadhyay
4/3/2020

(PROJECT INVESTIGATOR)

Dr. RUPAK MUKHOPADHYAY

Assistant Professor

Department of M B T

TEZPUR UNIVERSITY

Napaam, Tezpur-Assam, 784028

Rupak Mukhopadhyay

(HEAD OF THE INSTITUTE)

Tezpur

Tezpur University

Napaam, Tezpur

M. V. S. S. S.
18/1/20

(FINANCE OFFICER)

Tezpur

Tezpur University

Napaam, Tezpur